MODIFICATION OF A PROSTATE CANCER NEEDLE-BIOPSY DEVICE

By

YIBO WANG

A THESIS PRESENTED TO THE GRADUATE SCHOOL
OF THE UNIVERSITY OF FLORIDA IN PARTIAL FULFILLMENT
OF THE REQUIREMENTS FOR THE DEGREE OF
MASTER OF SCIENCE

UNIVERSITY OF FLORIDA

2024

To my family

ACKNOWLEDGMENTS

I would give thanks to my advisor and committee members, Dr. Greenslet and Dr. Tang, for their enduring support and insightful academic advice throughout my thesis. I would also acknowledge all Nontraditional Manufacturing Laboratory members for their help with my past years studying, especially in some fields that I am not familiar with. Additionally, the University of Florida Department of Mechanical & Aerospace Engineering receives my gratitude for their guidance on my thesis writing. Finally, I want to thank my family for their love and support.

TABLE OF CONTENTS

page

LIST OF TABLES

Table page

LIST OF FIGURES

Figure page

LIST OF ABBREVIATIONS

3D	Three dimensional
AC	Alternating current
ASA	Acrylonitrile styrene acrylate
CB	Carbon brushed
CPR	Counts per revolution
DC	Direct current
EMF	Electromotive force
ISR	Interrupt service routines
PCB	Printed circuit board
PLA	Polylactic acid
PSA	Prostate-specific antigen
PPR	Pulses per revolution
RPM	Revolutions per minute

Abstract of Dissertation Presented to the Graduate School
of the University of Florida in Partial Fulfillment of the
Requirements for the Degree of Master of Science

MODIFICATION OF A PROSTATE CANCER NEEDLE-BIOPSY DEVICE

By

Yibo Wang

May 2024

Chair: Greenslet, Hitomi Yamaguchi
Cochair: Tang, Xin
Major: Mechanical Engineering

One of the symptoms of prostate cancer is a malignant tumor, which can spread to other parts of the human body. Due to the rapid growth of cancerous cells, the cellular structure of prostate tissue is compressed, which causes cancerous tissue to be stiffer than healthy tissue. Needle-biopsy procedures, regarded as less invasive than open surgical biopsy, are used to extract tissue samples for cancer diagnoses. An aspiration-assisted end-cut coaxial needle biopsy device was introduced to improve biopsy performance. This device uses a vacuum created by a syringe to hold the sampled tissues in place, hence improving the tissue yield of the test. Recently, a hand-held end-cut needle biopsy device was developed based on the previous concept, and the feasibility of collecting large tissue samples with less sample distortion than commercially available biopsy devices was demonstrated. However, when the tissue sample was stiffer, the coaxial needle would be hard to extract due to the insufficient force, and even deflected in the worst case. The needle-insertion speed of the developed device was also much lower than commercially available biopsy devices. The needle throw length, which determines the tissue sample length, could not be simply adjusted. Therefore, the objective of my research is to refine the previously

developed device to include a more powerful motor to produce smooth, fast needle movement. In addition, an encoder will be integrated to the device for a customizable needle throw length. Furthermore, a current sensor will be included to detect the stiffness changes in the tissue.

CHAPTER 1
INTRODUCTION

In this chapter, the diagnostic methods of prostate cancer and the common devices currently available on the market will be discussed. Then the Aspiration-Assisted Needle Biopsy process based on this study will be explained in detail. In the end, the previous work on hand-held Biopsy Device V2.6 and research objectives will be introduced.

1.1 Prostate Cancer and Diagnosis Devices

Prostate cancer is a kind of malignant tumor of the prostate that can spread to other parts of the human body, especially the bones and lymph nodes. Prostate cancer may be asymptomatic in the early stages, but in later stages, symptoms can be pain and blood urinating. It has been the second most frequent malignancy in men worldwide, counting 1,276,106 new cases and causing 358,989 deaths in 2018 [1,2]. The etiology of prostate cancer still remains unknown, but it is known that the risk factors are highly related to age, family genetics, diet, and environmental carcinogens and so on. Although prostate cancer is very common, it is not as deadly as other cancers, especially in its early stages. According to the research from L. Egevad, prostate cancer with Gleason score 4-5 has about 18 years disease-specific mean survival and only 4.5 % mortality rate [3]. In fact, the mortality rate of prostate cancer varies widely in the world, which may be related to regional differences in the level of medical care. What is clear, however, is that the mortality rate of prostate cancer increases with age, with nearly 55% of deaths occurring after age 65 [2].

Early screening of prostate conditions can effectively prevent the occurrence and deterioration of prostate cancer. Results shows a 20% reduction in the rate of death

from prostate cancer among men offered screening for prostate-specific antigen (PSA) [4]. Contemporaneously, many methods have been developed for prostate screening, such as sonoelastography [5] and microscopic imaging [6]. After screening, biopsy will be conducted to extract prostate tissue samples from men who are at high risk for prostate cancer. Needle biopsy is considered to be the safest and most effective way to collect tissue samples. It is also a less invasive way rather than open surgical biopsy for evaluating suspicious changes.

At present, there are many kinds of needle biopsy devices on the market, like Biopince, Maxcore, etc. Their market prices also vary widely, ranging from $200 to $2,000. Most of them use an end-cut or side-cut needle to collect tissue samples. Figure 1-1 shows the difference between two kinds of needle. The end-cut is a hollow cylinder while the side-cut has a notch in the same that is used along with an outer cannula to store and retain tissue. These biopsy instruments use different dynamic systems to drive the needle like spring-loaded or motor-driven. Normally, biopsy devices are compatible with kinds of coaxial biopsy needles and these disposable needles can be replaced after collecting. They mainly set a depth reference by placing different markers to control the needle throw length. Although biopsy devices vary in size, they can drive a needle for a throw length around 30mm [7]. However, the actual sample length that can be obtained is often less than the needle throw length. Besides, they all have an ergonomic handle with a forward trigger to control the biopsy procedure.

1.2 Aspiration-Assisted Needle-Biopsy Procedure

Barnett et al. proposed a vacuum-assisted end-cut biopsy needle [8]. It consisted of an 18-gauge external needle with an inner stylette retracting system. This system creates a vacuum inside the needle to help suck the tissue sample into the space

between the external and inner needle. However, the over vacuum effect decreased the maximum efficiency. At the same time, excessive suction also stretched or compressed the tissue samples during extracting. In the worst case, it even distorted the shape of samples or broke the samples. To maximize the extraction of samples, a new aspiration-assisted needle biopsy procedure was developed. The biopsy procedure generally consists of four steps: insertion, cutting, holding, and extraction [9].

Figure 1-2 (a) shows the first step of this biopsy procedure. An end-cut coaxial needle will be inserted to the target position. After reaching the position, the motor of biopsy device will be activated and only the external needle moves forward at a constant speed, cutting through the tissue to get sample, while the internal stylette remains stationary. During the cutting process, a vacuum will be generated in the syringe barrel as shown in Figure 1-2 (b). This vacuum holds the extracted sample inside the external needle instead of sucking the tissue sample out of the lesion. As soon as the external needle gets stopped as shown in Figure 1-2 (c), a block will be inserted to prevent the external needle from moving relative to the stylette. Then the sample will be held tightly and ready for removal from the tissue. In the final step as Figure 1-2 (d) showing, the needle will be removed from the tissue. At that time if the motor is activated reversely, the sample inside the external needle will be expelled.

1.3 Previous Work

As discussed in Section 1.2, the aspiration-assisted needle-biopsy procedure can be used to effectively extract the tissue sample. However, it needs to be conducted through a large apparatus, named Coaxial Needle Biopsy System. Considering the size of the system, it seems to be impossible to use in the field for physicians.

To overcome the issue, a handheld needle biopsy device shown as Figure 1-3 was developed by Roy Araya and Zachary Tupper. The device was powered by a Pololu 6-Volts Micro Gearmotor with 2.0-kilogram centimeter stall torque and 450 revolutions per minute (RPM). A lead screw with a diameter of 3 mm and a pitch of 2.5 mm was connected to the motor. Accordingly, a 3D printed polylactic acid (PLA) lead nut was applied to the lead screw so that it would carry the flange of syringe to move. The lead nut had a permanent magnet embedded into the bottom surface to trigger the Hall Effect sensors as limit switches. Also, A small ATSAMD21E18 microcontroller and a DRV8836 motor driver were used to control the motor. Both were also integrated into a printed circuit board (PCB) to reduce the wiring inside the housing. When the lead nut reached its limiting position, the Hall Effect sensors would send the signal to the microcontroller to stop the motor. Meanwhile, the housing of the handheld device was ergonomically designed for easy use.

A new version of the handheld device was further developed by Roy Araya, Dane Ungurait and Keegan Bess. As shown in Figure 1-4, both PCB and microcontroller were replaced by an external breadboard circuit and an Arduino Uno board. Another change was that Hall Effect sensors were replaced by a current sensor. With the current sensor, the device had a new function of real-time current detection. The syringe nut would stop automatically when it hit the wall at the maximum needle throw length. At that time, the current would spike into the stall current. Once the current value reached the stall current, the motor would be shut down by our controller and reverse the rotation direction for the next time operation.

After that, Dane Ungurait continued to improve and modify the biopsy device. He made a new version of biopsy device for testing purposes. The major change was that the device housing became less ergonomic. Figure 1-5 shows a black flat box became the housing of the device. The rectangular design made it a better fixture in the sample collection test. Furthermore, the syringe was placed on a syringe nut moving along a linear guide rail. The rail would hold the syringe barrel running as smoothly as possible when the needle was cutting or extracting.

Although the handheld device was well developed by researchers from the University of Florida, there is still some room for improvement. According to the handheld device developed before, the needle throw length controlled by the Hall Effect sensor and current sensor was unprogrammable and hard to adjust. One side, the Hall Effect sensor was fixed to a position and sent the signal to the microcontroller only when the lead nut crossed the specific position. On the other side, the current sensor and sensor program only captured the stall current to stop the motor, which means the throw length only had two statuses: maximum or zero.

Another limitation was the power of the device. Due to the lack of torque provided by the medium-power motor, when the stiffer sample was biopsied, the coaxial needle was shown to be difficult to cut and extract, and even deflected in the worst case. Under the situation, the yield of tissue extracted from the biopsy procedure was dramatically reduced and even showed an increased zero biopsy rate.

In practice, the difficulty with diagnosis is that early-stage prostate cancer has few symptoms. However, due to the rapid growth of cancer cells, the cellular structure of prostate tissue is compressed with lost collagen as shown in Figure 1-6. This causes

cancerous tissue to behave differently from healthy tissue. The varying tissue stiffness can serve as an indicator of whether cancer is present. If tissue stiffness affects the torque required of the motor, it may be possible to detect changes in tissue stiffness by measuring the current to the motor in the device during the biopsy procedure.

1.4 Research Objectives

To solve the problems raised above, the research objective is to develop a new version of handheld biopsy device, which has a customizable needle throw length and a higher power to conduct the biopsy procedure more smoothly. Meanwhile, the biopsy device will also be developed to have a function of detecting tissue stiffness change. The goal is that the needle throw length will be precisely defined by a new motor control method, or any new electronic components. The handheld biopsy device can collect stiffer tissue samples with a larger cutting force applied by motor-driven mechanism. Furthermore, tissue stiffness change can be observed from current change, and there is a quantifiable relationship between them.

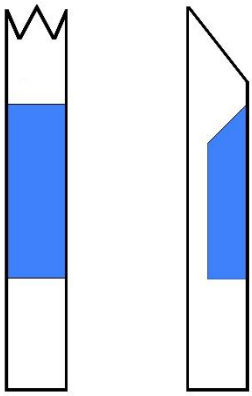

(A) (B)

Figure 1-1. End-cut needle and side-cut needle. (A) End-cut needle with tissue (blue) inside. (B) Side-cut needle with tissue (blue) inside.

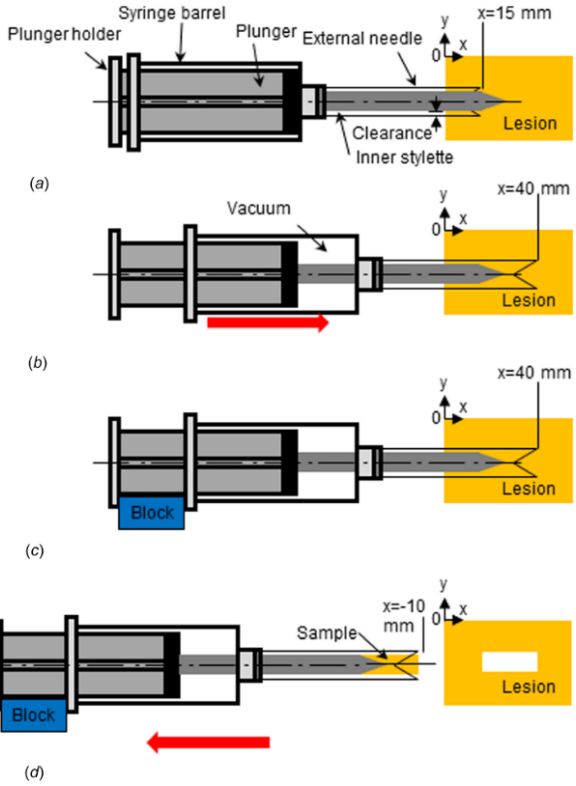

Figure 1-2. Aspiration-Assisted Needle-Biopsy procedure. (a) Insertion. (b) Cutting. (c) Holding. (d) Extraction. [9].

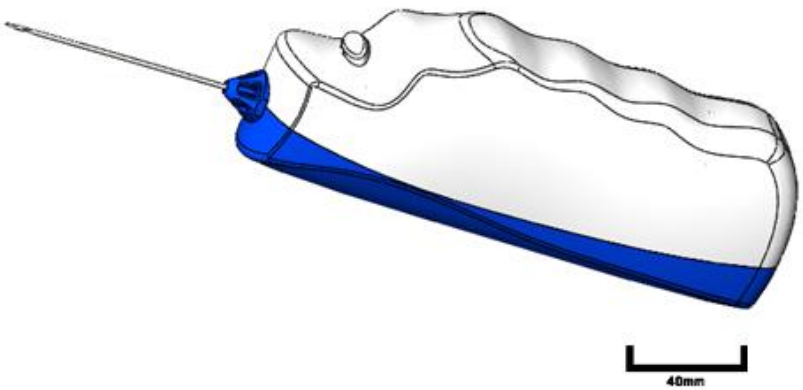

Figure 1-3. CAD Model of Ergonomic Handheld Biopsy Device.

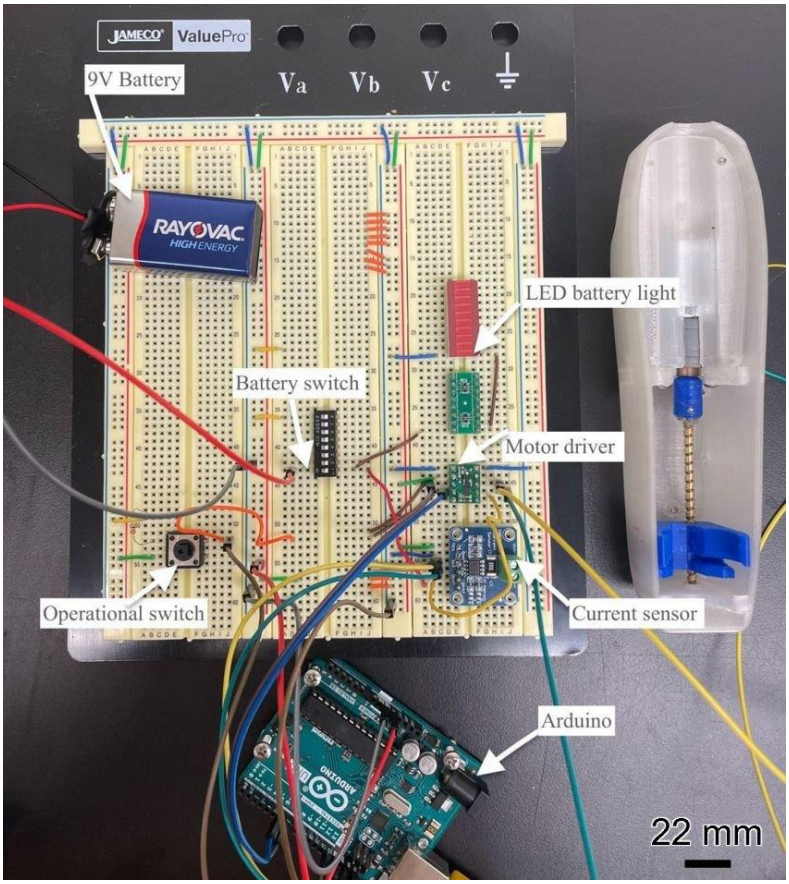

Figure 1-4. Breadboard Circuit and Handheld Device. [10].

Figure 1-5. Schematic of Biopsy Device V2.6. Figure courtesy of Dane Ungurait.

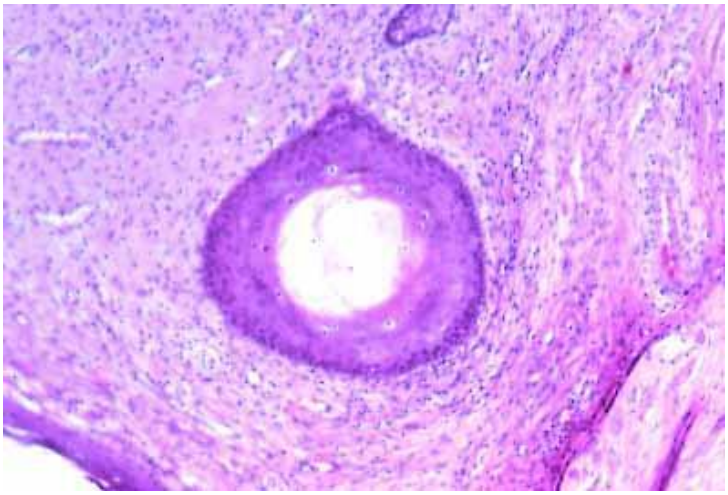

Figure 1-6. Prostate cancer tissue. [11].

CHAPTER 2
DEVICE REFINEMENT WITH HIGH POWER GEAR MOTOR

In this chapter, the power upgrade for the biopsy device will be discussed. Relatedly, the refinement of the components and stall current control system will also be introduced. Furthermore, the device performance will be examined through conducting gelatin collection test manually.

2.1 Part Refinement

There are five components that have been updated since the previous version: power supply, high power gear motor, motor driver, housing, and syringe nut.

2.1.1 Power Supply

Figure 2-1 shows the power supply of the previous version of device. It was a Duracell Coppertop Alkaline Battery. It could provide 9 V for rated voltage, which was enough for the old gear motor used before. It is suitable for a wide range of high-use devices.

Due to the change of high motor power, the voltage requirement is increased to 12 V. Therefore, an ALITOVE DC Power Supply Adapter Transformer was bought to supply 12 V direct current (DC) for our high-power motor. To use this power supply, a power cord was stripped to connect the electrical outlet shown as Figure 2-2. It can convert the 110 V alternating current (AC) to 12 V DC and output at most 120 W power.

2.1.2 High Power Gear Motor

Figure 2-3 shows the motor used before. It was chosen as 31:1 Metal Gearmotor 20Dx41L mm 6V Carbon Brushed (CB), which can only run under 6 Volts and provide torque at most 2 kg-cm. The shaft of this motor is 18 millimeters long and 4 millimeters wide. The max power is 2.3 Watts and RPM is 450 at no-load. According to the previous

biopsy test results, this motor could operate under 7.4 V and 5V but failed at 3.3 V (unable to recycle). Besides, it can not provide enough torque to run biopsy procedure with a standard syringe. Therefore, a corresponding modified syringe with less friction and vacuum effect was made to reduce the load for the motor [10]. Also, when the tissue became stiffer, zero biopsies would occur unexpectedly because it could not take more than 25 N to drive the syringe.

To increase the power of the gear motor, a higher power metal gear motor (11 kg-cm stall torque, 12.5 mm shaft length, 4 mm shaft diameter) was chosen to replace the old one. As shown in Figure 2-4, this new version motor can provide at most 8.9 W power. Meanwhile, the rated voltage of the higher power gear motor is 12 V and maximum rotational speed is 300 rpm.

At that moment, improving the torque supplied by the motor was prioritized over the speed of the motor, which means that the lower rotational speed is acceptable. The only thing that needs to be noticed is that the high-power gear motor can provide about five times the torque than the previous. This ensures that the biopsy device has plenty of power to drive the coaxial needle cutting the stiffer tissue in the test.

2.1.3 Motor Driver

As shown in Figure 2-5, the motor driver applied on the old version of biopsy device was DRV8838, which was an ideal driver for small motors that run on low voltages. The input of this driver is 5 V, and supply voltage is limited to 11 V. Accordingly, the motor driver can not run the high-power gear motor at full power and speed.

Therefore, the DRV8838 was replaced by G2 High-Power Motor Driver 24v13, shown as Figure 2-6. It can be clearly seen that the pin distribution on the driver is

different from the previous one. The maximum voltage for this driver is 40 Volts so it can drive the high-power motor now. In addition, it also has a current detection function, once the H-bridge is driving, the voltage output from the CS pin can be read by connecting to the controller then using a formula to calculate the current.

2.1.4 Device Housing

The next thing that will be discussed is the device housing changes. Figure 2-7 shows five major updates for the new version of biopsy device housing. Firstly, the new casing creates larger room for the new motor. The room size used to be 54mm long by 34mm wide and 47mm deep, but now it has become 68mm long by 42mm wide and 49mm deep, which is big enough to put our new motor. Additionally, due to the reason that the biopsy device was designed for standardization, the modified, loose syringe is going to be replaced by a 20 mL standard BD Plastipak syringe with an outer diameter of 21.25 mm. Accordingly, the dimensions of groove on the side wall and mid wall were adjusted to fit the new syringe better. Furthermore, some removable doors and windows were added to the housing, so that we can easily install the motor and other parts. Moreover, the linear guide rail was no longer an independent part, and it has been integrated into the bottom housing. The total length of slot in the guide rail is around 52 mm, which can produce at most 39mm for needle throw length. Finally, a slider module was also added to customize the needle throw length, matching with two windows to cover it. The module consisted of a block plate and two M5 screws with nuts and the length of this module is 60 mm in total. Once the two screws were put on the rail and close the window, then the operator would adjust the block plate to the target position, which could block the syringe nut to get the desired throw length. After that, two nuts on both sides would be used to sandwich the block plate as Figure 2-8 shown.

2.1.5 Lead Screw and Syringe Nut

The lead screw used before was made of copper. It was a M5 lead screw with 50 mm length and 3 mm pitch. Some flaws were found in the actual operation of this lead screw (see Section 2.2.1 and 2.2.2 for details). Furthermore, after several tests, it was found to be badly worn due to metal fatigue. Therefore, we replaced it with a new M3 stainless steel lead screw with 50 mm length and 0.5 mm pitch. It showed good strength in the biopsy test. Besides, the increase of pitch also improved the speed of needle insertion/extraction.

Due to the change of standard syringe, the syringe nut will also need to be adjusted to fit the syringe better. The diameter of this new syringe is 21.25 mm which is 1mm smaller than the old one. But it has a larger flange, with a size of 25.3 width and 38.7 mm length. Therefore, the new syringe nut was designed with lower thickness and a better arc shape. Also, the change of lead screw also requires changes of threaded hole on the syringe nut. To fit the M3 lead screw and increase the strength of inner thread, the 3D printed thread must be replaced. Therefore, a copper threaded thermal insert was applied into the syringe nut shown as Figure 2-9. According to the motor's speed-torque curve from Polulu official website [12], the copper thermal insert can withstand more than 3.8 kg-cm torque during the gelatin test.

2.2 Refinement of Syringe Barrel Motion Control

In this section the development of device control methods will be introduced. The prior control method is chosen as same as the old version device, which is the stall current control. The advantage of the current signal switch is that it is very simple to code and easy to control, and it can reach the maximum needle throw length very quickly. In addition, only an external current sensor was required to control the whole

biopsy procedure. However, the stall current control had limitations and did not show a good performance in the biopsy test. In the end, the manual control was chosen.

2.2.1 Motion Control with Stall Current

Stall current is the current drawn at maximum value when the motor is producing maximum torque but unable to rotate. It is either because it can't accelerate further or malfunctions. In an ideal situation, when the plastic syringe nut reaches its limiting position at the largest needle throw length, it is supposed to hit the wall and stop. In that case the motor can not rotate anymore due to angular position limitations. Meanwhile, the current crossing the motor will spike into the stall current, and the stall current value will be detected as a switch to stop the motor.

But at the same time, it also has many serious issues, especially when the motor was replaced with a high-power motor. The most serious issue is that the stall current with more powerful motor is increased to a relatively high value, which is impossible to reach for our device. In past tests, when the syringe nut reached its limiting position, the larger torque will force the lead screw to cut the inner thread on the syringe nut, causing the thread failed. Once the inner thread failed, the motor would continue idling and never stopped.

One reason is that the inner thread is not strong enough due to the 3D printed material issue, which is acrylonitrile styrene acrylate (ASA). Another reason is that the forward force is much larger than we expected. To demonstrate this view, the forward force provided by the new motor can be calculated and the result is that it was far beyond expectations.

First, the torque can be given as the equation shown below, where η is the transmission coefficient, *T* is the rated torque of the motor, *F* is the forward force on the syringe nut, *P* is the pitch of lead screw.

$$\eta \times 2\pi T = F \times P \tag{2-1}$$

According to the previous force measurements, the forward force generated by the old motor $F_1 \approx 20$ N; Lead screw pitch P_1 = 3 mm = 0.03 cm; Stall torque of the old motor T_1 = 2.0 kg·cm = 19.61 N·cm. Using equation 2-1, the transmission coefficient can be obtained as η = 0.0048.

The assumption is that the transmission coefficient η is a constant. The stall torque of high-power motor is T_2 = 11.0 kg·cm = 107.87 N·cm; New lead screw pitch P_2 = 0.5mm = 0.05cm. Similarly, the updated forward force generated by motor F_2 can be obtained as F_2 = 65.07 N.

Since the operation speed will stay constant, the forward force three times larger than before should be sufficient to drive the needle inserting a more rigid tissue sample. As shown in Figure 2-10, this excessive force kept pushing the nut forward into the solid wall and caused a jam when the nut exceeded its limiting position. After that the lead screw distorted and cut the inner thread on the plastic syringe nut, causing the motor to idle.

Another finding is that jams occurred more frequently when the lead screw was wiggling. A reasonable guess is that the wiggling creates a small offset between the thread on the lead screw and syringe nut, that makes a bad fitting. This kind of jam was well fixed as reducing wiggling by replacing the slot of the lead screw.

2.2.2 Stop Current Settings and Manual Control

To avoid over collision happening, the idea is to set an indicated current value, which is also called stop current, to stop the syringe nut from crossing the limiting position. Therefore, a program was written to judge whether the collision happens. Once the syringe nut crosses the limiting position, the motor is subjected to increased resistance, inducing a rise in current detected by the motor driver. Before rising to the stall current, the stop current signal can be used as a flag to control the motor. Normally, the stop current can be set as just a little bit larger than the operating current.

Figure 2-11 is a flow chart showing how the stop current control works. First, the operator clicks the button to start the procedure. Once the current exceeds the indicated current value, the motor will shut down. At that time if the operator clicks the button again, the motor will run reversely and change direction.

Table 2-1 records the maximum operating current and stop current values under different conditions. All the current data came from the current sensor integrated on the G2 24v13 motor driver. Due to the limited resolution of this current sensor, there is always an initial offset (50 mA) in the test. The first row explains the condition of tests. Initially, the test was conducted without a syringe and a needle with a 0.94 mm diameter stylette, after that added the syringe, then followed by the needle. From Table 2-1, it can be easily seen that the rated stall current of this high-power motor is 5.0 A, which is almost four times larger than the operating current. That’s another reason why the rated stall current can not be used to control the procedure as discussed in the previous section. All stop current settings always follow the principle of being slightly larger than the maximum operating current.

However, when using the stop current control to conduct a sample collection test, another thread issue occurred. As the syringe nut went towards the bottom of the syringe plunger, the inside thread was subjected to torque and broke. In fact, once the operating current exceeds 1.65A, the plastic thread would fail without any jam occurring. The initial thought was the failure was due to the material (ASA) of the 3D printed syringe nut, which is very fragile fitting with the brass lead screw. But this situation did not improve after replacing the inner thread with threaded thermal insert. The brass thermal insert showed varying degrees of wear as well when the motor current reached the stop current. A reasonable guess is that the high torque provided by the high-power motor will inevitably break the thread if the syringe nut exceeds the limiting position.

Therefore, to conduct the collecting test, the manual control had to be used to stop the motor. The manual control means that the operator will start or stop the syringe motion manually by pushing a button on the breadboard circuit. At the same time, he needs to decide the stop timing through visual inspection to achieve the desired needle throw length, which will inevitably lead to some errors.

2.3 Device Performance Test

After these modifications discussed before, device performance tests were conducted. The main goal of this test is to collect gelatin samples under manual control, using both the standard and modified syringe combinations with different inner stylettes.

2.3.1 Experiment Setup and Conditions

The gelatin collection experiment was set up as shown in Figure 2-12. On the left was the 7g/100mL concentration gelatin sample stored in a plastic test tube. There were two green marks on the tube made as a sign to help the operator control the stop timing manually. This tube was held by a black fixture through screwing down four screws on

the top. Then the whole fixture was fixed to the table by a C-clamp. On the right was our biopsy device. The total needle throw length was set to 25 mm with 10 mm initial penetration. Two groups of tests had been conducted under manual control by our biopsy device to investigate the device's performance. All tests were conducted with a standard BD syringe and fixed the syringe with different configurations. Meanwhile, two inner stylettes with different diameter were used to collect the gelatin sample. The aim of tests is to find the influence of different fixing configurations and different inner stylettes.

2.3.2 Results and Discussion

From Table 2-2, the first finding is that the syringe should be at least covered by the tape during the test. In the tests, sponges and tape were clearly observed to reduce vibration of the syringe. It also demonstrates that the sponge and tape were the most reliable fixing condition because the sample length and mass obtained under this condition were the most stable. The second finding is that the stylette with 1.04 mm diameter collected more samples than the 0.94 mm one. One side, the collected sample length was much closer to our needle throw length when using larger diameter stylette. On the other side, the 0.94 mm inner stylette did not collect the sample for full needle throw length, which might be due to excessive vacuum effect and friction.

From Table 2-3, the same tests were conducted but both standard and modified syringe. The modified syringe had lower friction for the gasket and lower vacuum effect, which was used to compare the influence of biopsy with different vacuum effect. In tests, only the 1.04 mm diameter inner stylette was used to collect samples. Additionally, the syringe was covered with a newly designed top handle shown as Figure 2-13. According to the experimental data, it can be seen that except for the

outlier of the 7th and 8th trial, the collected sample length using modified syringe is very close to needle throw length which is 25mm. Figure 2-14 shows an example of a collected sample under manual control. Besides, using a modified syringe did not change the sample length and mass significantly. It also means that the lower vacuum effect and friction is acceptable in the biopsy procedure.

In conclusion, the test results showed that the high-power motor provided enough torque to operate a standard BD syringe (20 mL) and conduct the biopsy procedure. Furthermore, the modified syringe also had enough vacuum to conduct the biopsy procedure.

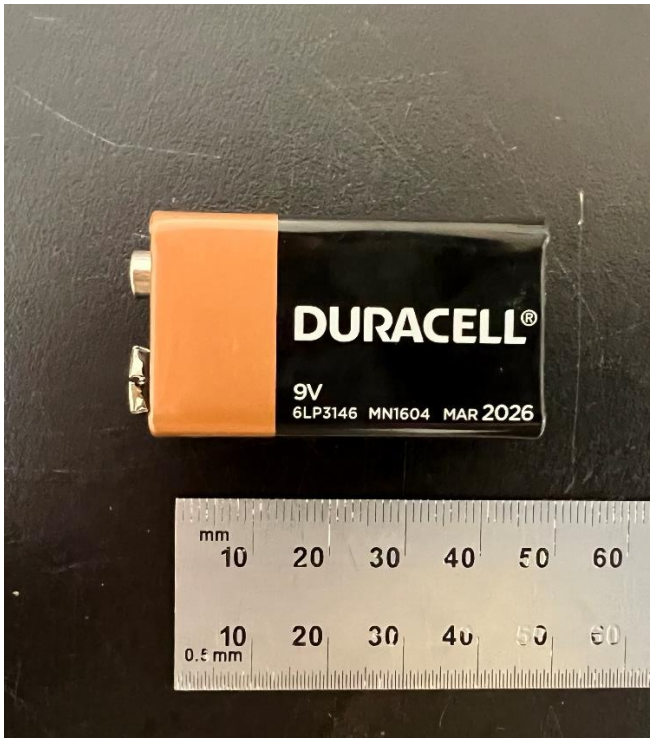

Figure 2-1. Duracell Coppertop 9 V Alkaline Battery.

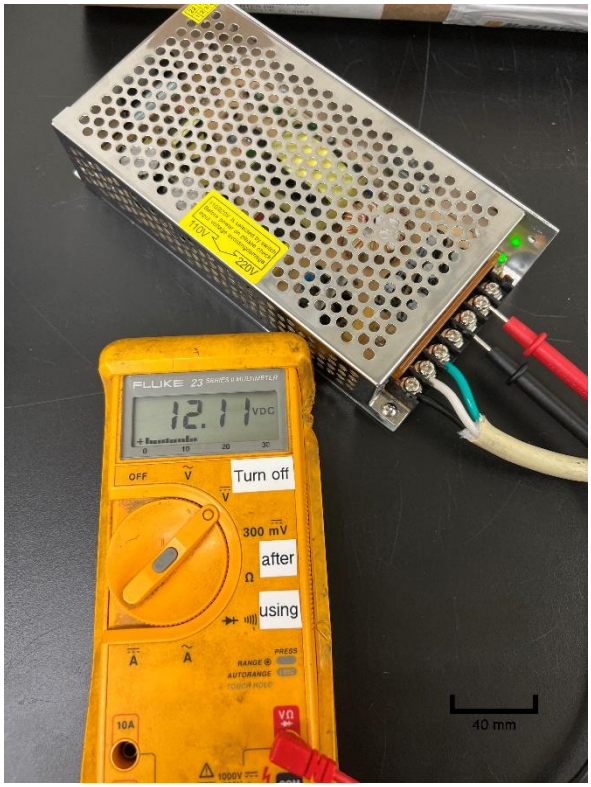

Figure 2-2. ALITOVE DC Power Supply Adapter Transformer. Rated voltage measurement of the power supply was 12.11 V.

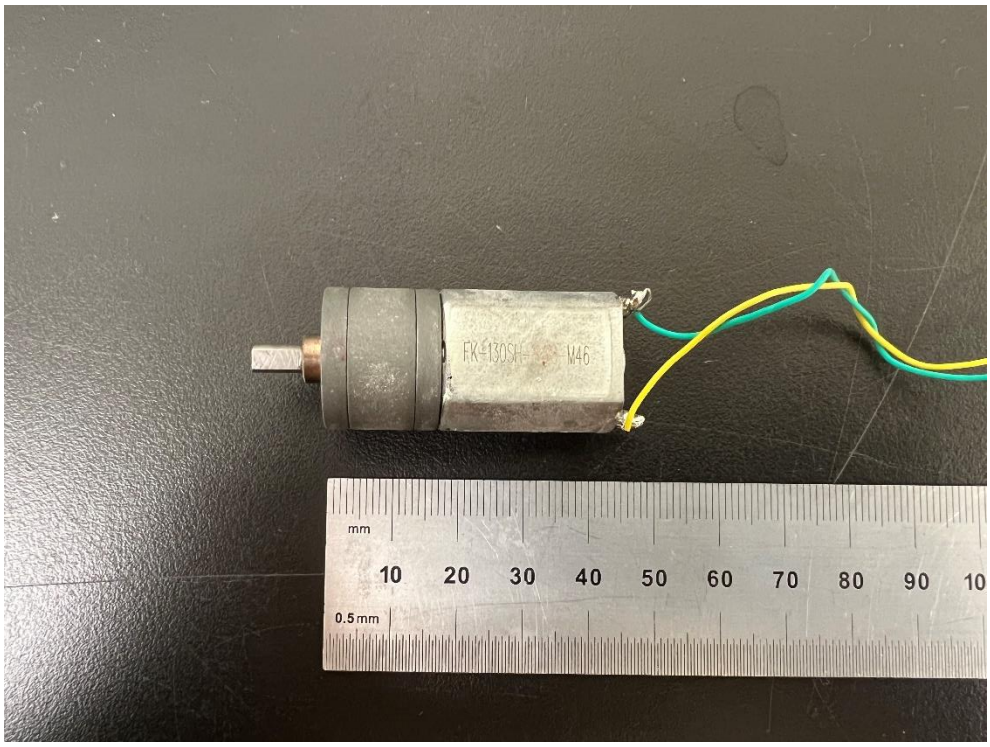

Figure 2-3. 31:1 Metal Gearmotor 20Dx41L mm 6V CB.

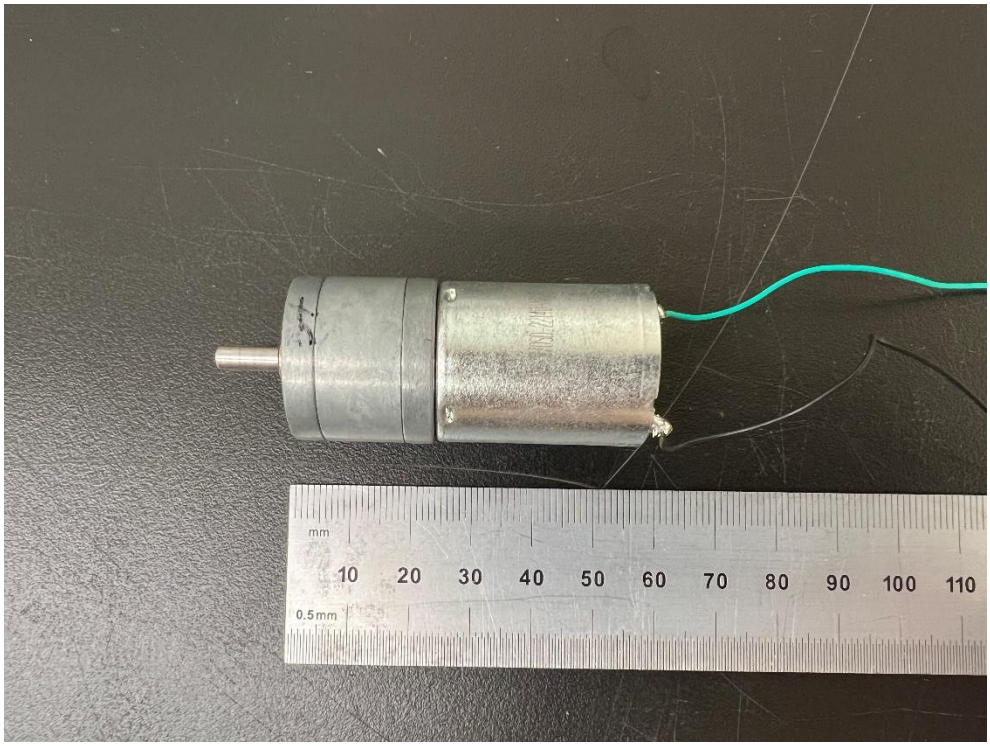

Figure 2-4. 34:1 Metal Gearmotor 25Dx52L mm HP 12V.

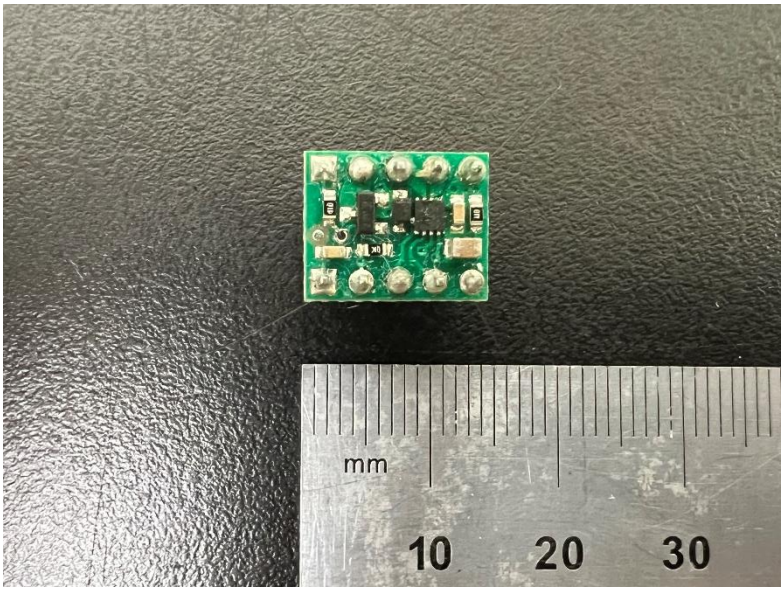

Figure 2-5. DRV8838 Motor Driver.

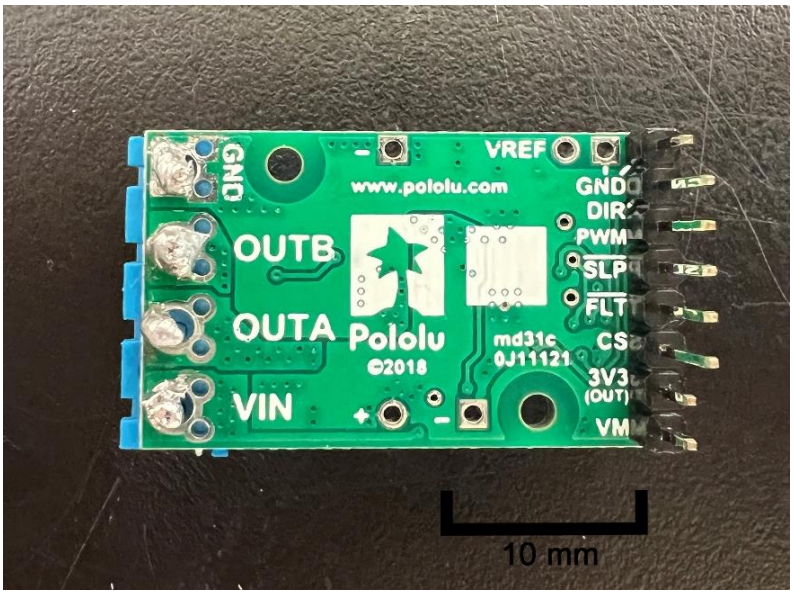

Figure 2-6. G2 High-Power Motor Driver 24v13.

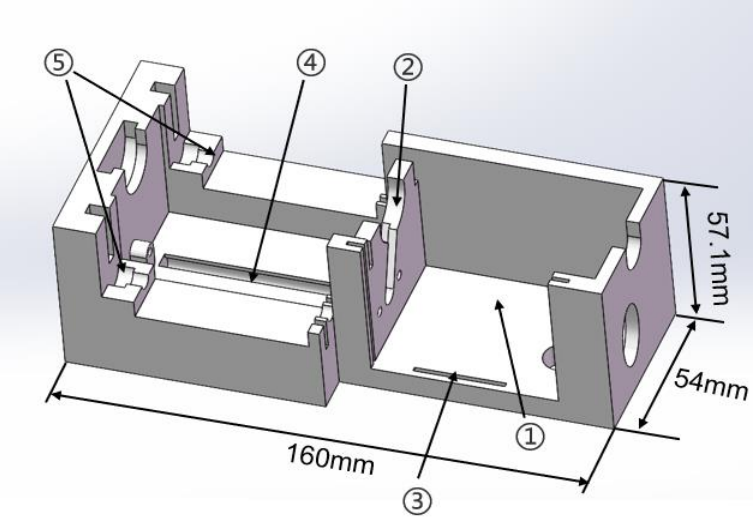

Figure 2-7. Biopsy Device housing CAD design.

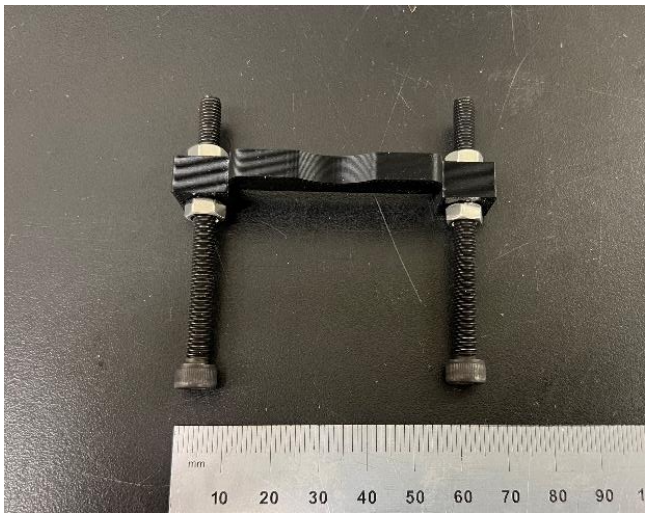

Figure 2-8. Slider module. The block plate is sandwiched between two nuts on both sides.

Figure 2-9. Threaded thermal inserted syringe nut.

Figure 2-10. The issue of syringe nut thread during the biopsy test. The brass lead screw cut through the inner thread when the nut stopped at the limited position. The orange spiral debris was the thread that has been cut by lead screw.

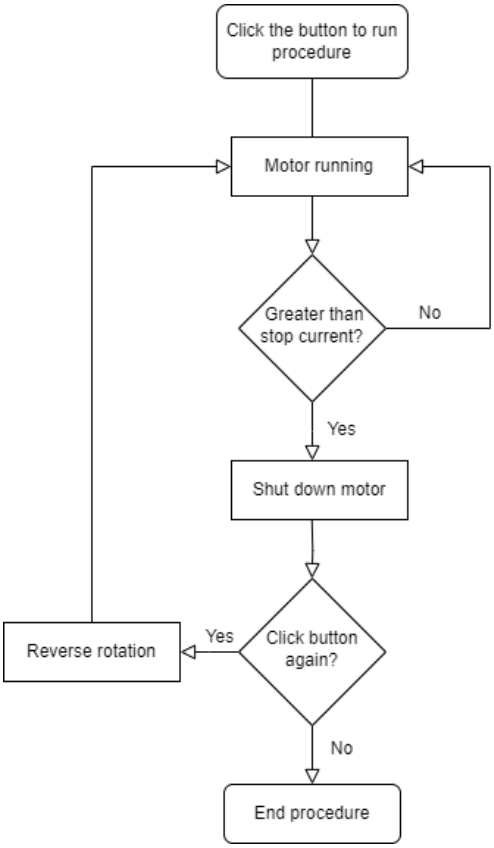

Figure 2-11. Flow chart of stop current control.

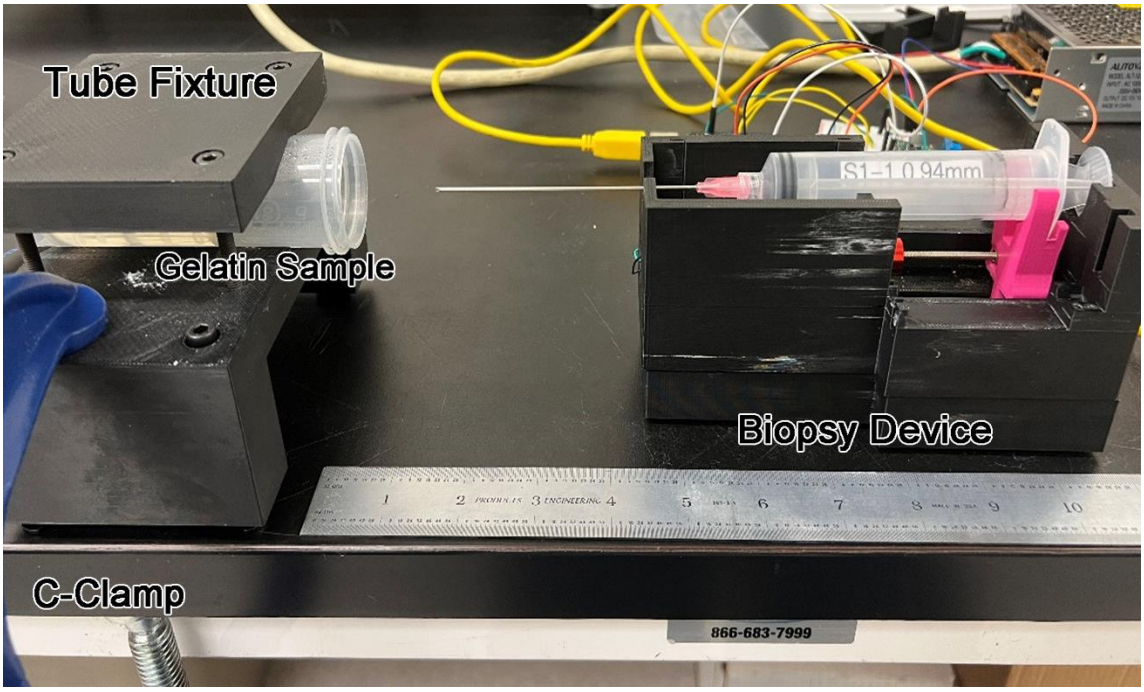

Figure 2-12. Schematic of the manual control gelatin collection experiment setup.

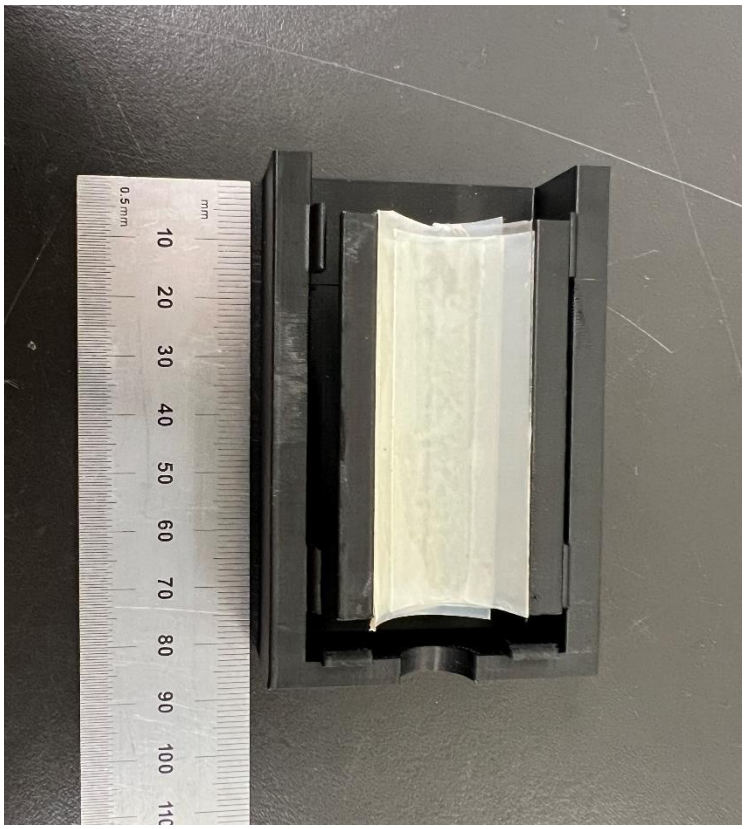

Figure 2-13. Top handle.

Figure 2-14. Collected tissue sample through manual control.

Table 2-1. Stop current values setting for the high-power motor. The stall current is 5.0 A.

Condition	Maximum operating current (A)[a]	Stop current (A)
No syringe and needle	1.04	1.28
Only syringe	1.22	1.41
Syringe and needle	1.41	1.65

[a] The initial offset is 0.92 A and the motor current is proportional to the motor driver CS pin output. Output voltage is about 40 mV/A plus a 50 mV offset.

Table 2-2. The gelatin collection test used two different gauge inner stylettes and a standard BD syringe under various fixed conditions.

Trial number	Inner stylette diameter (mm)	Gelatin concentration (g/100mL)	Sample length (mm)	Sample mass (mg)	Fixed condition
1	0.94	7	16.2	16.53	No sponge or tape
2	0.94	7	17.1	17.85	Only tape
3	0.94	7	17.0	18.23	Sponge and tape
4	1.04	7	26.2	20.51	Sponge and tape
5	1.04	7	26.8	20.97	Sponge and tape
6	1.04	7	25.8	19.84	Sponge and tape

Table 2-3. The gelatin collection test used both the standard syringe and modified syringe with a 1.04 mm diameter inner stylette.

Trial number	Inner stylette diameter (mm)	Gelatin concentration (g/100mL)	Sample length (mm)	Sample mass (mg)	Syringe type
1[a]	1.04	7	26.2	20.51	Standard syringe
2[a]	1.04	7	26.8	20.97	Standard syringe
3[a]	1.04	7	25.8	19.84	Standard syringe
4	1.04	7	25.2	21.83	Modified syringe
5	1.04	7	25.8	22.74	Modified syringe
6	1.04	7	24.8	21.63	Modified syringe
7[b]	1.04	7	23.0	18.24	Modified syringe
8[b]	1.04	7	19.8	16.84	Modified syringe

[a] These three trials were conducted under a sponge and tape fixed condition, while others were under a top handle fixed condition. But both fixed conditions produce similar stabilizing effects on the syringe.
[b] Two trials can be considered as outliers. During the test, gelatin samples were exposed to air for too long then softened.

CHAPTER 3
DEVICE REFINEMENT WITH PRECISION SYRINGE-BARREL MOTION CONTROL AND TISSUE-STIFFNESS DETECTION FUNCTION

In this chapter, it will show how the encoder controls precision syringe barrel motion. Some of device components are added or modified to support a new tissue stiffness detection function. To verify the availability of new function, the relationship between the current and tissue stiffness will be investigated.

3.1 Part Refinement

To support the new function development, refinement was performed on the parts of the biopsy device. The major part refinement in biopsy device will be shown as five components: modified syringe, fixture, motor and encoder, and current sensor.

3.1.1 Modified Syringe

As discussed in the previous chapter, a standard BD syringe has been demonstrated to provide over vacuum effect for the biopsy procedure. Therefore, a modified syringe was made to replace the standard syringe in the previous biopsy test. As shown in Figure 3-1, the modified syringe has all components as same as the standard BD syringe, except for the gasket. To reduce the friction and vacuum effect of syringe, the gasket was edged to have a smaller diameter and wrapped with frictionless tape to reduce friction with the barrel wall.

3.1.2 Fixture Design

In order to conduct biopsy tests on the linear stage device, a fixture for adjusting the position of the biopsy device was designed, which is shown as Figure 3-2. It was made of a 200 mm long, 150 mm wide acrylic plate as a platform. Four 60 mm long M5 screws and T-nuts served as support on 80/20 aluminum extrusions. There are also six positioning M4 bolts to help fix the biopsy device on the platform.

This fixture can move along the extrusion by T-nuts that were sliding in the slot. Once the platform moved to the desired horizontal position, then the user would screw down the M5 bolts and fixed the platform. This fixture reduces the wobbling and increases the stability of the device in biopsy test.

3.1.3 Motor with Encoder

To achieve the customizable needle throw length, a 12 V Pololu gearmotor with a 48 counts per revolution (CPR) incremental encoder was purchased as Figure 3-3. When the motor shaft rotates, the encoder converts the rotational position into an analog signal for impulse output. Normally people use both channels of the encoder, then the rotational direction can be determined by the sequence of square wave offset. Also, through calculating the number of rising edge and falling edge of both channels, the number of pulses can be obtained by diving the number of edges by four.

In practice, using only one channel is also possible and coding will be much easier than using two channels. However, it will reduce the encoder resolution by a factor of 4, which results in 12 CPR. The error analysis of using one channel will be discussed in more detail in Section 3.2.2.

3.1.4 Current Sensor

In order to measure the current during a biopsy test, the device needs to be improved to have a current sense function. There are two options for current sensors. The first option is to use the sensor integrated on the motor driver. The motor driver has a current sense output function. CS pin outputs a voltage proportional to the motor current when the H-bridge is driving. The advantage of using motor driver sensor is that it is simple to use and does not require additional circuit modifications.

Another option is to integrate an independent current sensor chip into our circuit and develop a new code for it. Figure 3-4 shows an INA219 current sensor chip which can be powered by the 5V pinout on the Arduino Uno board. It can withstand a maximum current of 3.2A. According to the stop current value obtained in Chapter 2, it can be found that the maximum operating current value can reach 1.41A when both syringe and needle are loaded. Therefore, it is reasonable to believe that 3.2A is a safe range even in tissue collection test. The advantage of using independent current sensor is that it has a good resolution of 100 μA, which means that it can figure out any slight current change during the biopsy test.

3.2 Refinement of Syringe-Barrel Motion Control Using Encoder

Using stall current control, the needle throw length could only be full range or zero. Then we try to set the needle throw length manually. However, since the stop timing needs to be determined by operator through observation, the precision of needle throw length is limited and fluctuating. Therefore, as we discussed in Section 3.1.3, a 48 CPR encoder was applied to the device to achieve precise syringe-barrel motion control, which also leads to a customizable needle throw length.

3.2.1 Time Interruption Function in Code

To count the rising and falling edges of both channels' outputs, it is necessary to ensure that the program always captures pulses from the rotary encoder. Ideally, our controller will never miss any pulses if it only performs this task. However, it also needs to perform other tasks most of the time, and a program that constantly reads the sensor lines for the encoder will become a huge burden for our controller. Therefore, time interruption can be used for making things happen automatically in programs and can help solve timing problems, including reading a rotary encoder, or monitoring user input.

In the Arduino IDE, one of the ways to realize the time interruption is to use attachinterrupt (). This function can interrupt the digital pins on the Arduino board when counting the rising/falling edges of both channels. The first parameter of this function is the number of the interrupted pin. It is worth mentioning that for the Arduino UNO R3 board, only pin 2 and 3 support this interrupt function. The second parameter is the interrupt service routines (ISR), which is code that will execute when an interrupt occurs. In our case, the ISR should be a code that counts the number of rising edges and falling edges. If only one channel is used to record the rotation, then the angular displacement will be defined as the motor rotating clockwise when a rising edge occurs, whereas the motor rotating counterclockwise when a falling edge occurs.

The final parameter is the interrupt mode, which defines the triggering of the interrupt condition. It's usually divided into four types: LOW to trigger the interrupt whenever the pin is low; CHANGE to trigger the interrupt whenever the pin changes value; RISING to trigger when the pin goes from low to high; FALLING for when the pin goes from high to low.

3.2.2 Error Analysis

In practice, the controller is unable to capture every single pulse accurately because data transmission takes time. Additionally, the interrupt function we used in the program may result in some error. For instance, to measure and update the real time angular position, the MsTimer2 function was used to set the time interval as 0.1s. Given the 48 CPR (=12 pulses per revolution (PPR) for one channel) and pulses number m in 0.1s, the real-time rotational speed ω RPM can be obtained every 0.1 seconds (update the output every 0.1 s) by the equation below:

$$\omega = \frac{m}{12} \times \frac{1}{k} \times \frac{1}{0.1} \times 60 \tag{3-1}$$

While the encoder provides counts in the gearbox instead of the motor shaft. It means that the pulse number needs to be divided by the gear ratio *k*, which is 34.014:1.

Similarly, we can define the required number of pulses *m* through the shaft revolutions *n*:

$$m = n \times k \times 12 \tag{3-2}$$

And *n* can be obtained by the expected needle through length *l* mm and lead screw pitch *p* mm:

$$n = \frac{l}{p} \tag{3-3}$$

Once ω is obtained, the error σ can be given as:

$$\sigma = \omega \times \frac{1}{60} \times 0.1 \times p \tag{3-4}$$

For our motor, the no-load performance of rotational speed ω is 300 RPM and lead screw pitch *p* is 0.5 mm, which means that it can produce a maximum error 0.25 mm for our needle throw length. This error will decrease as the rotational speed decreases.

3.2.3 Experimental Conditions

Compared to the previous gelatin test, the encoder control gelatin collection experiment was conducted on our linear stage device, which made the device more stable and consistent. The total experiment set up was shown as Figure 3-5. The tube with gelatin sample was held by the tissue holder on the linear stage device. Meanwhile, the biopsy device was placed on the newly designed fixture that can slide along the aluminum extrusions to adjust the position of the needle tip. In the experiment, the initial

needle penetration depth was determined as 10 mm and the total needle throw length was set to 25 mm. The needle would be moved to the target position by moving the device and fixture together. After reaching the position, M5 bolts on both sides were screwed down and the casing would get fixed, then the gelatin collection experiment was ready to conduct.

3.2.4 Results and Discussion

Five trials of gelatin collection tests were conducted under encoder control and the results are shown in Table 3-1. One of the collected samples as an example is shown in Figure 3-6. The head structure was displayed as slightly bulged in the proximal of gelatin sample. Compared with the previous samples collected by a standard syringe, the head structures were smaller possibly due to a weaker vacuum effect using the modified syringe. The five trials all had a relatively perfect length which was much closer to the needle throw length compared to the previous manual control results.

In fact, some samples could not be precisely measured. In practice, we needed to use tweezers to remove the collected sample from the coaxial needle after each trial. Especially when the gelatin was taken out of the refrigerator, it would begin to soften quickly due to rising temperature after minutes of test. Some samples may have been accidentally deformed while extracting from the needle using the tweezers. Moreover, the fragile gelatin seemed more likely to fracture during the extraction process. In the worst case, the broken samples will be pieced back together for length measurement, thus affecting the final measurement result.

In conclusion, it demonstrates that the collected sample length was well controlled by our encoder. The obtained gelatin samples length is at most 2.3 mm longer or 1.6 mm shorter than the setting needle throw length.

3.3 Tissue-Stiffness Detection Function

As mentioned in the first chapter, mechanical properties of cells and extracellular matrices are critical determinants of oncogenic transformation. Due to the rapid growth of cancer cells, cellular structures of prostate tissue are compressed with losing collagen. This causes cancerous tissue to be stiffer than any normal healthy tissue. Therefore, one way to diagnose prostate cancer is to measure the Young's modulus as an indicator of stiffness change. To detect the stiffness changes in the tissue, one way is to use our encoder alongside a current sensor. By measuring current values of the motor at different needle positions, the resistance of the needle will be fed back, which can figure out the tissue stiffness. Normally, the resistance to the tip of the needle will increase when the needle sticks into a stiffer tissue sample. Then the larger torque will be required by the motor, which leads to a higher current value through the motor recorded by our sensor.

3.3.1 Experiment Setup and Conditions

Like the previous encoder control gelatin collection tests, the tissue stiffness detection tests were also conducted on the linear stage device with fixture. The only setup difference is that an INA219 current sensor chip was added into the biopsy device's circuit. It was directly connected in series with the positive terminal of our motor to record the current through the motor when the PWM was set to the maximum output. Furthermore, because the alternative experimental scheme is to use the current sensor

integrated on the motor driver, it does not require us to change the circuit design especially.

To investigate the change of stiffness in the tissue sample, some layered gelatin samples with various stiffness were made as Figure 3-7. They consisted of three portions of 20mL gelatin with different concentrations (7, 14, 21 g/100 mL). According to the compression tests conducted by Dane [10], it showed that the gelatin's stiffness increased with increasing concentration. Young's modulus indicates the macroscopic stiffness of material, and Young's moduli of the 7, 14, 21 g/100 mL gelatin was 18 kPa, 20 kPa and 31 kPa respectively. Additionally, it is obvious that there were boundary layers between each of the different concentration gelatin. The gelatin sample was also fixed by the tissue holder on the linear stage device in the test.

The goal of the experiment is to find the availability of using a current sensor to detect the tissue stiffness change. It will demonstrate if the sensor on the motor driver can be used to detect the stiffness change by conducting layered gelatin sample test. If the sensor has enough resolution to identify the stiffness change, then it is effective. However, if the driver's sensor does not work well, the independent current sensor INA219 will be considered as an alternative method.

3.3.2 Relationship between Current and Tissue Stiffness

To verify whether or not the motor driver sensor has enough resolution to detect the sample stiffness change, the layered sample test has been conducted. The initial penetration for the coaxial needle was set to 5 mm to the layer between 7 g/mL and 14 g/mL concentrations gelatin. Also, the total needle throw length was set as 20 mm. During the gelatin test, the sensor integrated on the motor driver will output an analog signal through CS pinout to our Arduino board shown as a voltage value, which can be

transferred to the real-time current crossing the motor. According to the Polulu official website [13], the output voltage is about 40 mV/A plus a 50 mV offset. After tests conducted, the detected current change was shown as Figure 3-8. In the first trial, a delayed peak was observed, representing larger resistance when the needle punctured into higher concentration gelatin. But this phenomenon did not appear in the second trial. It demonstrated that the change in the current due to stiffness change is not dramatic (less than 50 mA). Due to the limited resolution of our driver's sensor, it can not figure out any small current changes.

Therefore, a more accurate sensor will be required as an alternative way. Using the INA219 sensor, current detection tests were successfully performed and the average current values under different conditions during the operation were recorded as Table 3-2, Table 3-3, and Table 3-4.

Table 3-2 shows average motor current values of five biopsy trials but with no gelatin sample collection. In the tests, only the modified syringe and the coaxial needle were attached to the device. This group was performed as a control group to measure the initial average current value in the biopsy procedure.

Since the high-power motor used was a brushed motor, it would inevitably produce some noise during the operation. However, according to the uncertainty analysis of the obtained data, it shows that these noises do not have a great impact on the confidence level of the data. The standard deviation and 95% confidence interval can be defined as below:

$$\sigma_c = \sqrt{\frac{\sum_{i=1}^{n_c}(x_i - \mu)^2}{n_c - 1}} \tag{3-5}$$

$$\mu \pm 1.96 \times \sigma_c \quad (3\text{-}6)$$

Substituting the experimental data into 3-5 and 3-6, the 95% confidence interval can be obtained as 535.84 ± 73.99 mA. Both the maximum (Trial 1) and minimum (Trial 5) values of the data are within the 95% confidence interval.

Another three groups of different concentrations individual gelatin tests were also conducted, and the results are shown as Table 3-3 and Figure 3-9. It is obvious that the average current value in the biopsy test decreased with the increase of gelatin concentration. One thing worth mentioning is that the higher the gelatin concentration was, the less sample would be obtained. At the same time, to verify whether the average current was proportional to the sample mass, a scatter plot was drawn as Figure 3-10, and the correlation coefficient of each individual gelatin test has been calculated. The correlation coefficients of the 7, 10.5, 14 g/100 mL group were -0.1408, 0.1657, 0.5193. It can be found that the correlation coefficients were not stable and increased with the increase of gelatin concentration. Therefore, the relationship between current and sample mass still remained unclear.

The same trend also applies to layered gelatin test as shown in Table 3-4 and Figure 3-11. When the needle inserted to the 14 g/100 mL gelatin, the average current recorded was around 200 mA lower than the current in case of sticking into 10.5 g/100 mL and 7 g/100 mL gelatin. Also, the average current for the 10.5 g/100 mL gelatin was approximately 100 mA lower than the 7 g/100 mL case. According to the compression tests conducted before [10], it is known that stiffness of gelatin increases with concentration. But when gelatin with a larger stiffness was biopsied, the average current value in the procedure was lower, which is a counter-intuitive conclusion.

3.3.3 Discussion

In order to understand the specific current variation trend, the throw length versus current data obtained by encoder and INA 219 will be plotted. Previously in Section 3.3.2, only average currents of the entire biopsy procedure were discussed. With data points recorded in the tests and linear interpolation, a more specific relationship between the motor current and stiffness will be investigated.

Figure 3-12 shows how the current changed in three groups of individual gelatin tests. It can be seen that when the coaxial needle initially collected the gel, there was a significant increase in the motor current. It is because the motor was in a starting stage. In the starting stage, the rotor accelerates from rest state. When the motor speed is zero, the end counter electromotive force (EMF) of stator is zero, so that the power supply bus voltage will be directly loaded to the stator resistance, resulting in a larger current. Correspondingly, there should also be a motor ending stage when the biopsy procedure finished, and the throw length almost reached 30 mm. However, because of the inertia of the motor rotation, it was impossible to stop immediately when the needle throw length reached its target length. And only the data with throw length between 0 and 30 mm were collected in the test, so no rapid current drop was observed there.

To study the current change when the motor is stably rotating, the data of 0-5mm and 25-30 throw length are removed. Then the relationship between the motor current and stiffness will be shown as Figure 3-13. Except from the starting and ending stages, it can be found that the current trend of different concentration of gelatin test is generally similar, and they all increase slightly with the increase of needle throw length. This makes sense because as the throw length increased, the contact area between coaxial

needle and gelatin sample also increased, which caused more friction and thus increased the motor current value.

Furthermore, for gelatin samples with different concentration (or stiffness), there was a significant shift in their curve. In terms of the overall trend, the 7 g/100 mL gelatin has the highest average current value, although it is not always larger than the current of 10.5 g/100 mL gelatin at every single data point. It is speculated that this may be due to electromagnetic noise. Also, the current values of 10.5 g/100 mL and 7 g/100 mL gelatin were generally higher than lower concentration gelatin or no gelatin case. These results were consistent with the conclusion obtained in Section 3.3.2.

The same trend also goes for the layered gelatin tests as shown in Figure 3-14. A very significant rise in the current can be seen in the test, which is entirely different from the slight rise observed in the individual tests before. One possible guess is that the current increase was due to the gelatin stiffness decrease.

Overall, it obtained the same conclusion as in Section 3.3.2: the larger the concentration of the tissue collected is, the lower the motor current will be. A reasonable guess to explain this counterintuitive phenomenon is that the gelatin concentration increases with an increased stiffness as well as a decreased viscosity. Figure 3-15 also helps illustrate this phenomenon: when the external needle penetrates the gelatin for collection, it is subject to three kinds of resistance. Two of them are the friction force and cutting force related to the gelatin viscosity, and the other is the puncture force related to the gelatin stiffness. However, since the needle is subject to much less puncture force than the sum of friction and cutting force in the biopsy procedure, the current increase caused by increasing the gelatin stiffness can not trade off the current

decrease by decreasing the viscosity, which results in a drop of current in measurement macroscopically.

In addition, Figure 3-16 can be used as another evidence to support the above views. Another layered gelatin made in a different order (7 g/100 mL—10.5 g/100 mL—14 g/100 mL), was put into collection tests and shown a trade-off trend in both 5-10 mm and 20-25 mm region. It means that the current value was larger when the tissue stiffness was small, and smaller when tissue stiffness was large. Compared with the blue line, which is a layered gelatin in the order of 14 g/100 mL—10.5 g/100 mL—7 g/100 mL, the orange line has a more stable current variation trend. It is consistent with our theory.

Figure 3-1. Modified syringe. The 0.99 mm diameter external stylette was also attached to the syringe.

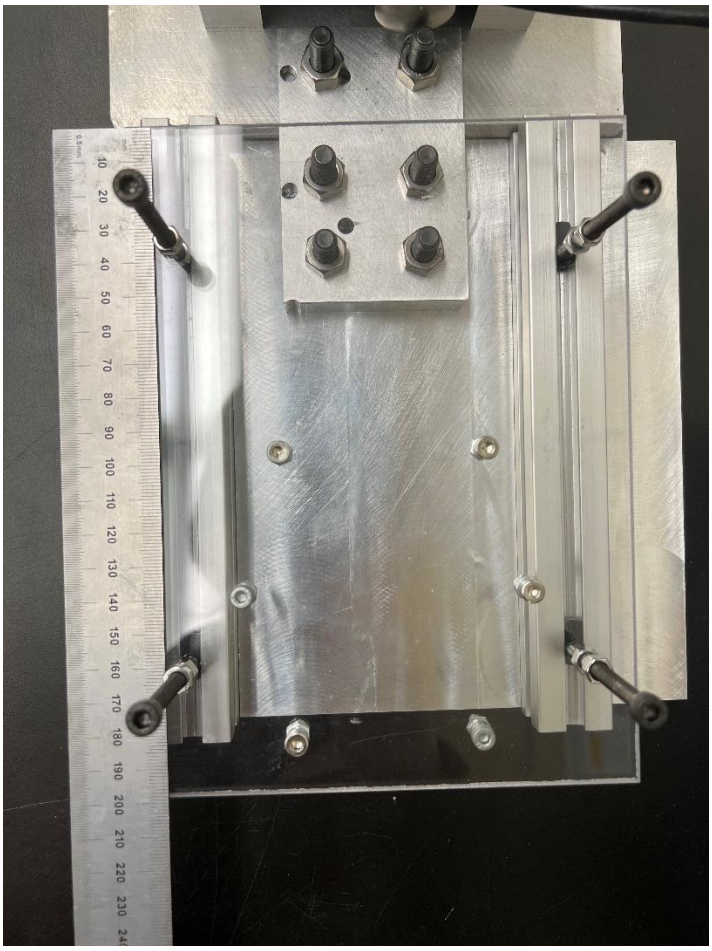

Figure 3-2. Fixture attached on the linear stage device.

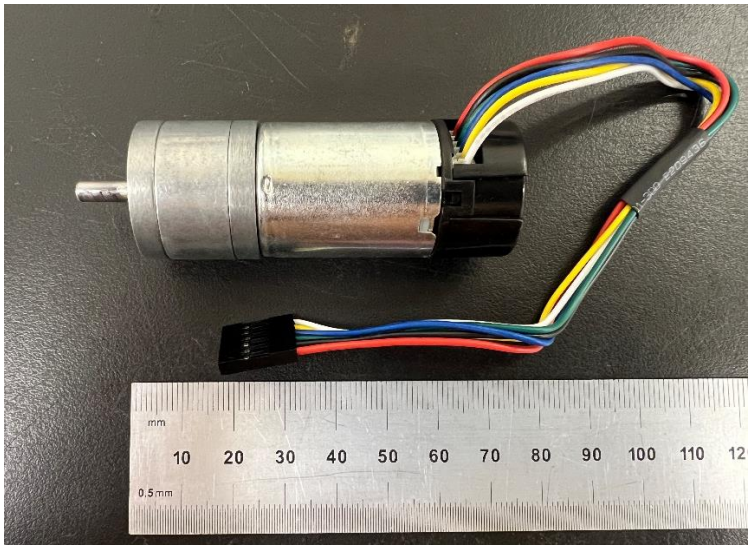

Figure 3-3. 34:1 Metal Gearmotor 25Dx67L mm HP 12V with 48 CPR Encoder.

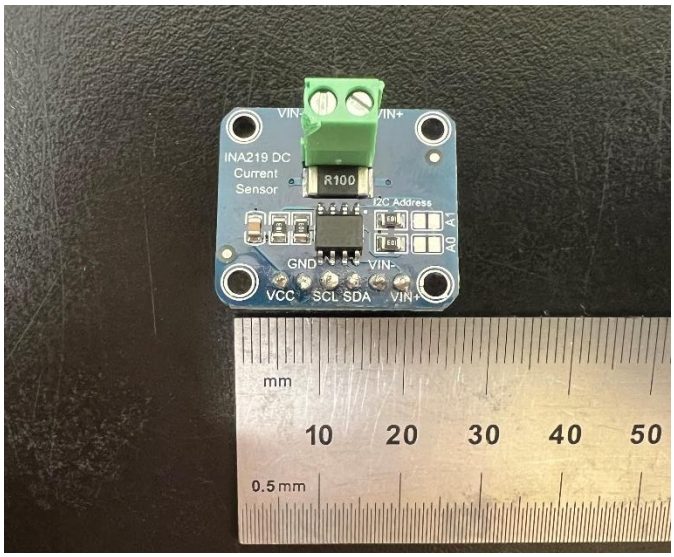

Figure 3-4. INA219 DC Current Power Supply Sensor.

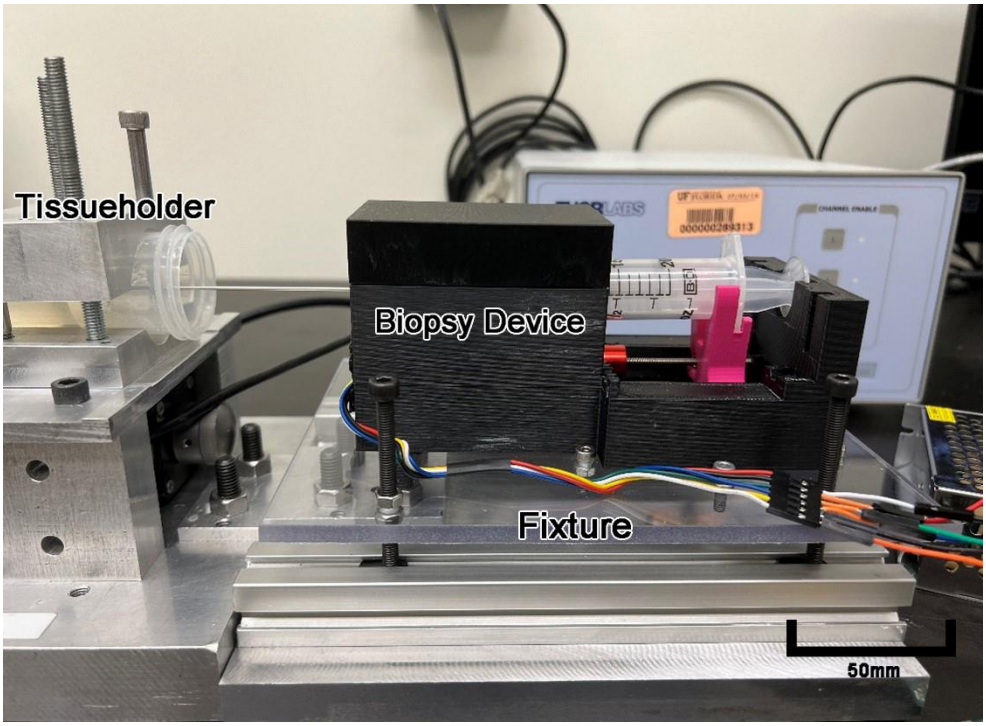

Figure 3-5. Schematic of the encoder control gelatin collection experiment setup.

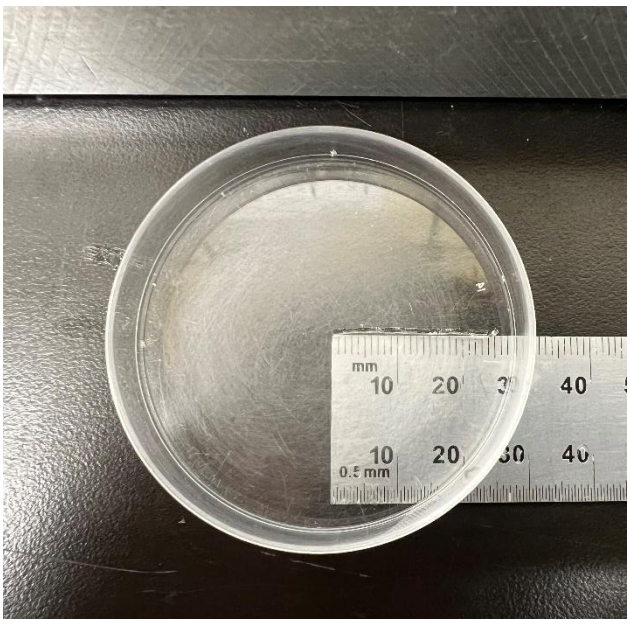

Figure 3-6. Collected tissue sample through encoder control.

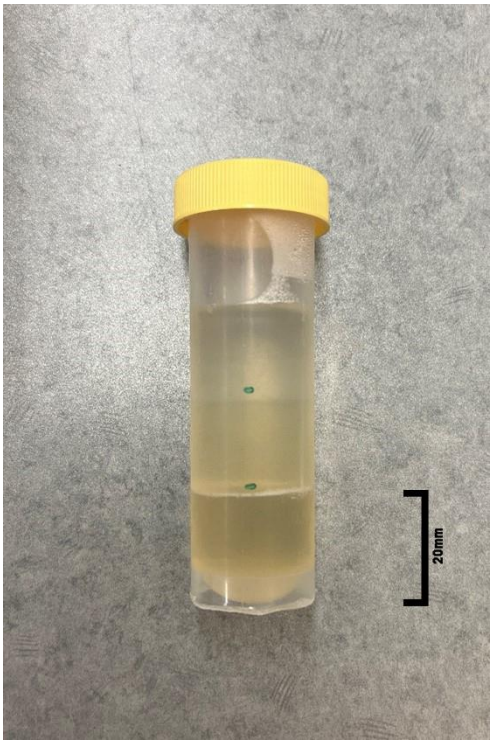

Figure 3-7. Layered gelatin with different concentrations: 7g/100mL, 14g/100mL, 21g/100mL (from top to the bottom).

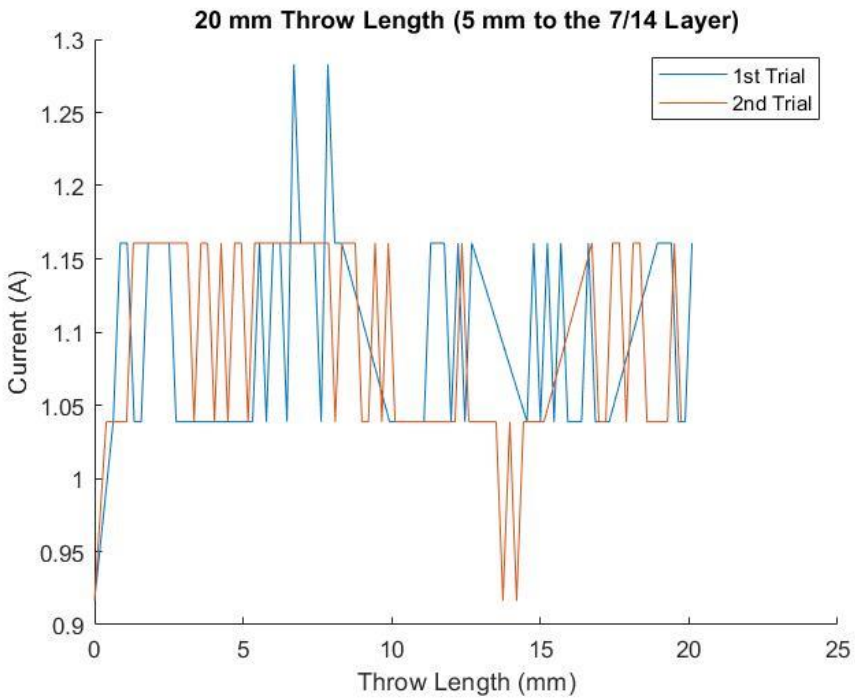

Figure 3-8. The motor driver detected the current change in the layer gelatin collection test.

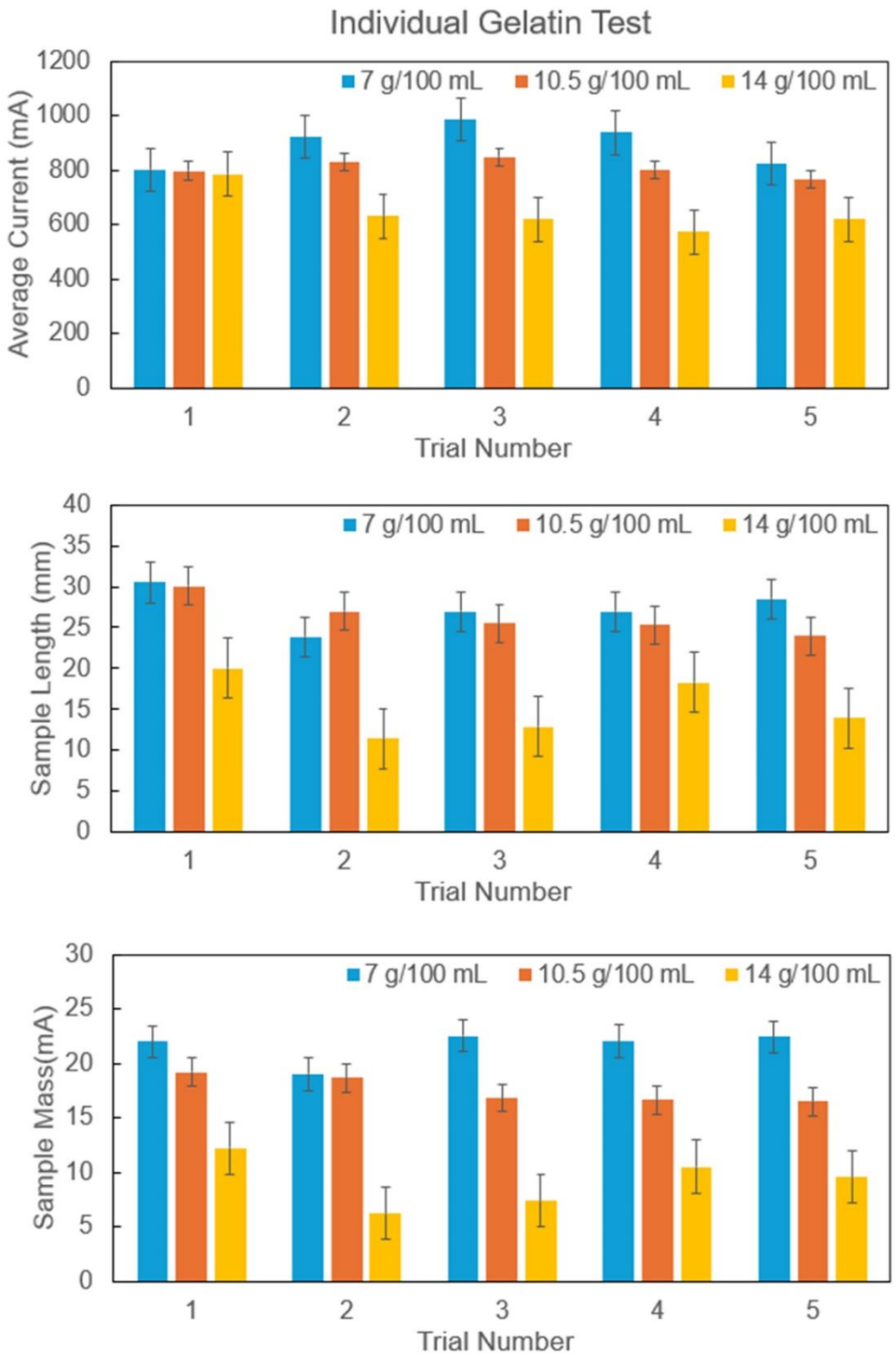

Figure 3-9. Recorded average motor current values during the tests for 7,10.5,14 g/100 mL individual uniform gelatin.

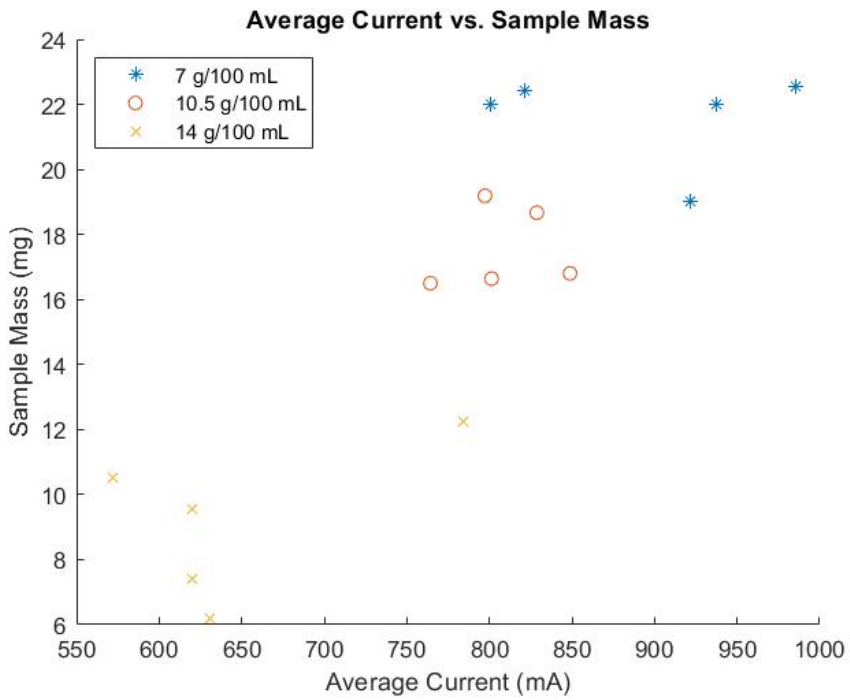

Figure 3-10. The scatter plot. It shows the relationship between the average current and sample mass.

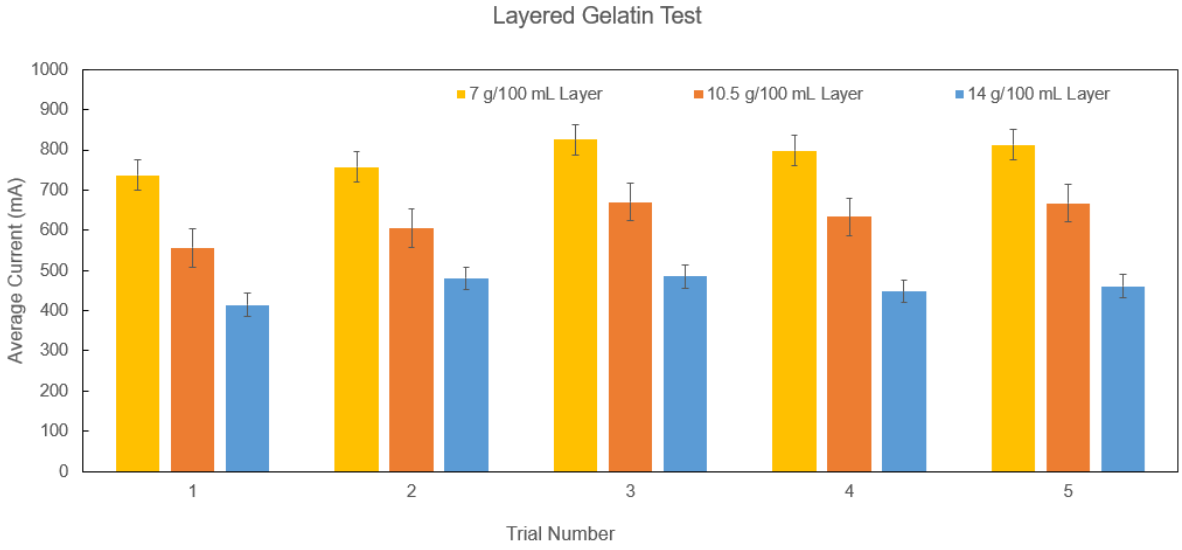

Figure 3-11. Recorded average motor current values during the tests for layered gelatin.

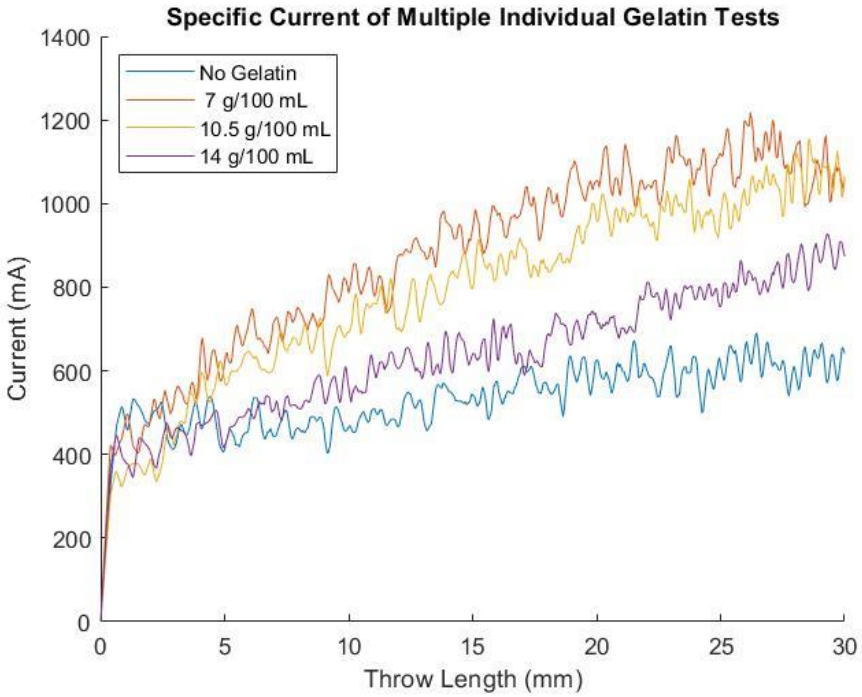

Figure 3-12. Current changes in individual gelatin collection tests. All data collected were the average of five trials and linearly interpolated.

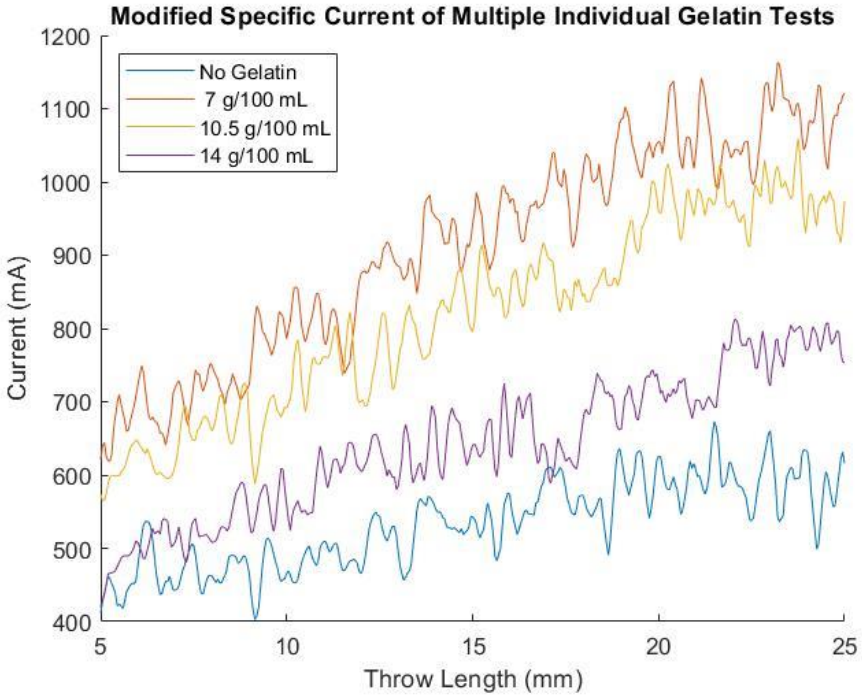

Figure 3-13. Modified current changes in individual gelatin collection tests. All data collected were the average of five trials and linearly interpolated. Data of first 5 mm and last 5 mm throw length has been removed.

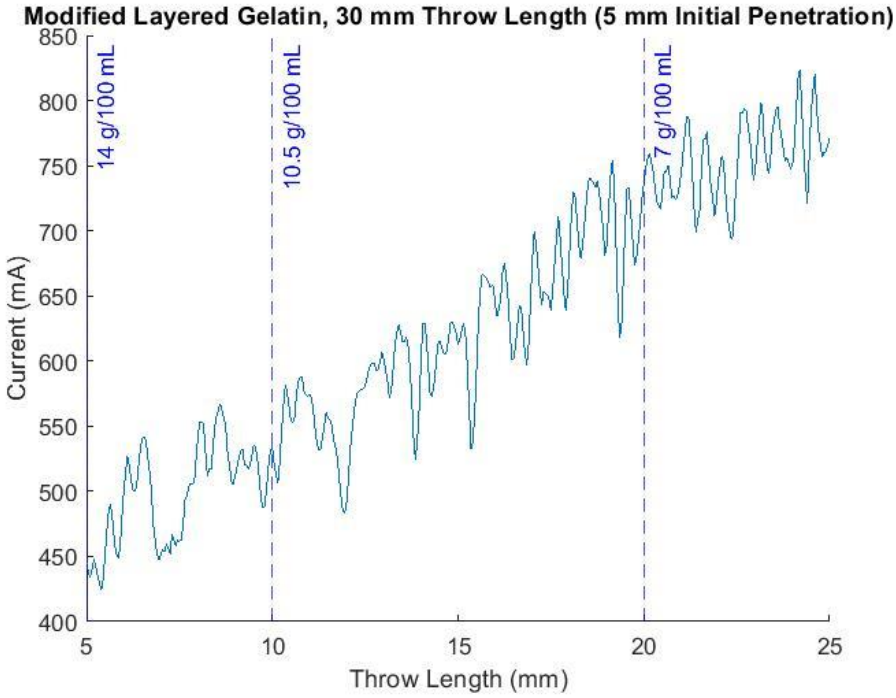

Figure 3-14. Current changes in the layer gelatin collection test. All data collected were the average of five trials and linearly interpolated. Data of first 5 mm and last 5 mm throw length has been removed. As needle penetrated into the layered gelatin, the order is 14 g/100 mL --10.5 g/100 mL—7 g/100 mL.

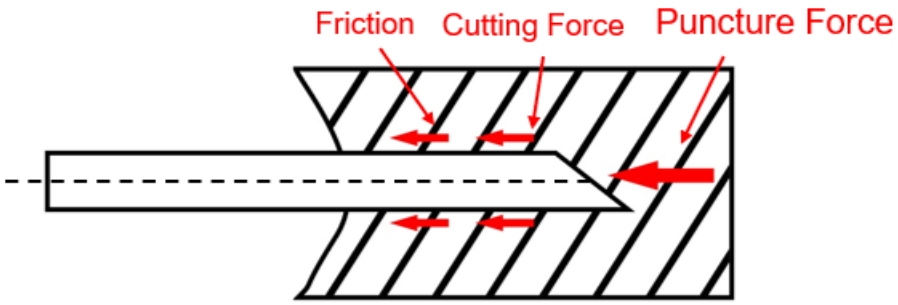

Figure 3-15. Schematic of resistance exerted on the needle. The large arrow represents the puncture force exerted on the tip, while the small arrows represent the friction and cutting force exerted on the contact surface.

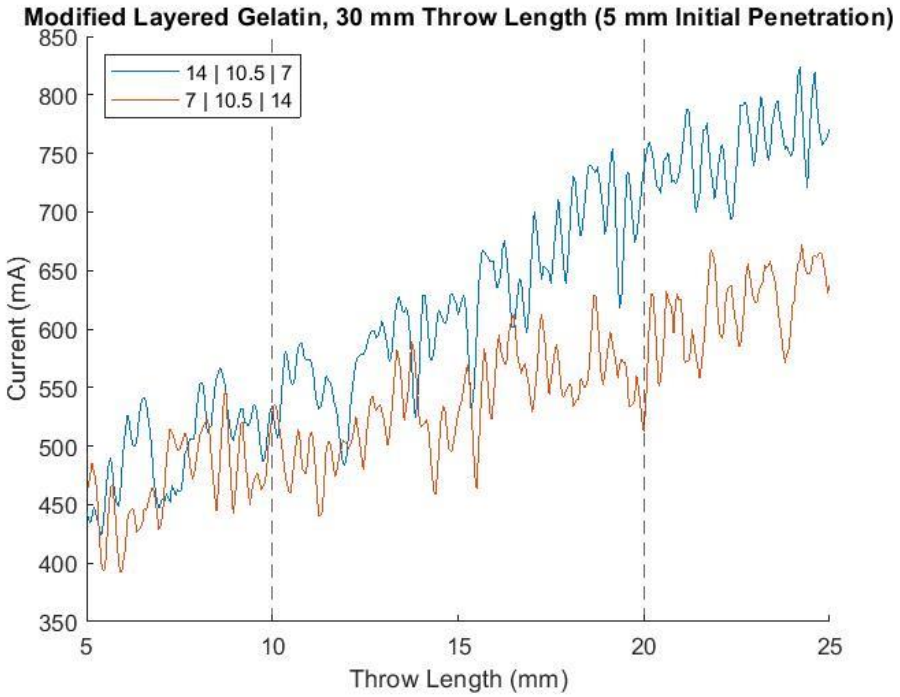

Figure 3-16. Current changes in two groups of layer gelatin collection tests. All data collected were the average of five trials and linearly interpolated. Data of first 5 mm and last 5 mm throw length has been removed. The needle penetration order of blue line is 14 g/100 mL --10.5 g/100 mL—7 g/100 mL, while the orange line is 7 g/100 mL --10.5 g/100 mL—14 g/100 mL.

Table 3-1. The 7g/100mL gelatin collection test. A modified syringe with a 0.99 mm inner stylette was used and all tests were conducted under encoder control.

Trial Number	Throw Length Setting (mm)	Sample Length
1	25	27.3
2	25	25.5
3	25	23.4
4	25	25.5
5	25	27.2

Table 3-2. Recorded average motor current values during the tests without gelatin sample. The initial needle penetration was 5 mm and total throw length was 30 mm.

Trial Number	Average Current (mA)
1	584.588
2	550.965
3	507.743
4	546.793
5	489.096

Table 3-3. Recorded average motor current values during the tests for 7,10.5,14 g/100 mL individual uniform gelatin. Five trials were performed for each gelatin configuration. The initial needle penetration was 5 mm and total throw length was 30 mm.

Trial Number	Gelatin Concentration (g/100 mL)	Average Current (mA)	Sample Length (mm)	Sample Mass (mg)
1		800.781	30.5	22.01
2		921.628	23.9	19.01
3	7	985.804	27	22.54
4		937.057	27	22.02
5		821.783	28.5	22.43
1		797.367	30.1	19.19
2		828.728	27	18.67
3	10.5	848.821	25.5	16.80
4		801.308	25.3	16.64
5		764.303	24	16.50
1		784.334	20	12.23
2		630.501	11.4	6.21
3	14	620.292	12.9	7.39
4		572.121	18.3	10.52
5		619.779	13.9	9.55

Table 3-4. Recorded average motor current values during the tests for layered gelatin. The initial needle penetration was 5 mm and total throw length was 30 mm. The layered gelatin consisted of three layers with 14,10.5,7 g/mL concentration in the order of penetration. Each layer of gelatin had a collectable thickness of 10mm.

Trial Number	Layered Concentration (g/100 mL)	Average Current (mA)
1		413.986
2		480.531
3	14	485.264
4		448.109
5		460.807
1		556.330
2		604.879
3	10.5	670.472
4		632.913
5		667.642
1		736.740
2		757.514
3	7	825.648
4		797.582
5		812.148

CHAPTER 4
CONCLUSIONS AND FUTURE WORK

In this chapter, it will show the conclusion of the research of biopsy device and some future work, like quantification of the relationship between the motor current and stiffness, and any potential improvement of the device.

4.1 Conclusions

Prostate cancer stands as a significant global health concern, with its prevalence and impact on male populations worldwide. Despite development in early screening methods and biopsy procedures, challenges persist in enhancing the efficiency and stability of diagnostic devices. The aspiration-assisted needle-biopsy procedure presents a promising method for sample extraction. However, the size of needle biopsy system has so many limitations, which have prompted the development of a handheld version of biopsy devices. The evolution of these devices highlights the ongoing efforts to make the handheld device more adaptable and reliable.

Nevertheless, existing handheld devices have constraints such as fixed needle throw lengths and limited cutting power, impacting their ability to extract diverse tissue samples effectively. Addressing these limitations, the research objectives aim to propel the development of a new version of a handheld biopsy device. The envisioned enhancements include a customizable needle throw length, more powerful motor, and the incorporation of a gelatin stiffness detection function.

In general, the major development and modification of the handheld biopsy device can be divided into a few points. First, the motor of the biopsy device now has been upgraded to have a higher power to extract the tissue sample. Furthermore, the use of a power supply provided an increased voltage to drive the high-power motor.

Second, updated electronic components like motor driver and independent current sensor were added to the circuit. Meanwhile, the housing design was also modified, including an enlarged space for the new motor, integration of the linear guide rail, and the addition of removable doors and windows. Also, the breadboard circuit was rebuilt and optimized to have a smaller layout. Third, an encoder was applied to the motor so that it could customize the needle throw length precisely. Fourth, an encoder-current sensor combined gelatin stiffness detection function was well developed. After individual and layered gelatin tests, it showed a trend that the higher concentration of the gelatin sample was collected, the lower the motor current would be.

4.2 Future Work

For future work, the most important thing is to quantify the relationship between gelatin stiffness and current. One of the two essential points is to eliminate electromagnetic noise from the output terminus of encoder. According to previous tests, the fluctuation of 100mA to 150mA brings negative effects on the observation of current change. The plan to solve this issue is to incorporate a high-pass filter into the circuit to eliminate noise. Another point is to separate the stiffness and viscosity effects, which means that puncture force and friction with cutting force measurements at the needle tip will be separated. One option is to use a cannula of the same diameter as the external needle [14]. The cannula is first inserted into the gelatin before the test, then the operator removes gelatin inside the cannula. After that the cannula will be removed and coaxial needle will be inserted into the hollowed-out hole to conduct the same collection test as before. This prevents the front side of needle tip from cutting the gelatin directly, and thereby preventing the puncture force occurring. In that case, the measured current

change will only depend on the friction and cutting force, which is mainly determined by the viscosity of gelatin.

In the long term, the handheld biopsy device will be developed with more functions. In practice, the biopsy device should be capable of stopping bleeding after penetration. One way to achieve that is adding an extra layer between the external needle and inner needle. The layer can store hemostatic material including fibrin, collagen, and cyanoacrylate. Another way is to heat the needle to stop bleeding like an endotherm knife. When the cells are heated to 60 °C~95 °C, the proteins can be denatured to achieve the purpose of ligation of blood vessels. Therefore, an external heat exchanger can be attached to the external needle for heating. An electronic thermometer will be added to the device to monitor the temperature at any moment.

APPENDIX A
BIOPSY DEVICE ARDUINO UNO MANNUAL CONTROL CODE

```
#include <Wire.h>
#include <stdio.h>
enum states {
  STANDBY,
  CUTTING,
  REMOVAL,
  EXITING
};

enum states deviceState;

const int button = 13;
const int DIR = 7; // analog
const int PW = 6; //digit  al
const int pwm = 0;
const int encoder_outputA = 2;
const int encoder_outputB = 3;
const int high = 255;

int buttonVal = 0;
int outputA = 0;
int outputB = 0;
void setup() {

  Serial.begin(115200);
  pinMode(button, INPUT);

  pinMode(DIR, OUTPUT);
  pinMode(PW, OUTPUT);
  pinMode(encoder_outputA, INPUT);
  pinMode(encoder_outputB, INPUT);


  deviceState = STANDBY;

  digitalWrite(DIR, LOW); // this will brake, regardless of what ph is
  digitalWrite(PW, LOW);

}

void loop() {
  // put your main code here, to run repeatedly:
```

```
buttonVal = digitalRead(button);
outputA = digitalRead(encoder_outputA);
outputB = digitalRead(encoder_outputB);
if(deviceState == STANDBY){
  if(buttonVal == HIGH){
    deviceState = CUTTING;
    digitalWrite(DIR, LOW);
    analogWrite(PW, 255);
    delay(100);
  }
}

else if(deviceState == CUTTING){
  if(buttonVal == HIGH){
    digitalWrite(DIR, LOW);
    digitalWrite(PW, LOW);
    deviceState = REMOVAL;
    delay(100);
  }
}

else if(deviceState == REMOVAL){
  if(buttonVal == HIGH){
    deviceState = EXITING;
    digitalWrite(DIR, HIGH);
    analogWrite(PW, 255);
    delay(100);
  }
}

else if(deviceState == EXITING){
  if(buttonVal == HIGH){
    digitalWrite(DIR, LOW);
    digitalWrite(PW, LOW);
    deviceState = STANDBY;
    delay(100);
  }
}
//Serial.print(deviceState);
//Serial.print(" ");
//Serial.print(volt);
//Serial.println(" ");
Serial.begin(115200);
Serial.print("OutputA:");
Serial.print(outputA);
Serial.print(",");
```

```
   Serial.print("OutputB:");
  Serial.println(outputB);
  delay(100);
}
```

APPENDIX B
BIOPSY DEVICE ARDUINO UNO ENCODER CONTROL AND CURRENT DETECTION CODE

```
#include <MsTimer2.h>
#include <Wire.h>
#include <stdio.h>
#include <Adafruit_INA219.h>
Adafruit_INA219 ina219;
enum states {
  STANDBY,
  CUTTING,
  REMOVAL,
  EXITING
};

enum states deviceState;

const int button = 13;
const int DIR = 7; // analog
const int PW = 6; //digit  al
const int pwm = 0;
const int encoder_outputA = 2; //must be 2 or 3 for arduino uno
const int encoder_outputB = 3; //must be 2 or 3 for arduino uno
const int high = 255;

volatile long ppsA = 0;
volatile long count = 0;
int m = 0;
int buttonVal = 0;
int outputA = 0;
int outputB = 0;

char a ='+';
char b ='-';
char c;
float velocity = 0;
float revolution = 0;
        float v(float n)
        {
          float vel = n/0.1/34.014/12*60;
          // ppr = 48/4 = 12
          return vel;
        }
        float revo(float m)
        {
          float re = m/12/34.014;
```

```
            return re;
        }
void flash()
{
float velocity = v(ppsA);
//Serial.print(velocity);
//Serial.println("RPM  ");
ppsA=0;
}

void setup() {
  Serial.begin(115200);

  if (!ina219.begin()) {
    Serial.println("can not find INA219 chip");
    while (1) { delay(10); }
  }

  uint32_t current;
  attachInterrupt(0,CountA, FALLING);
  MsTimer2::set(100, flash);
  MsTimer2::start();

  pinMode(button, INPUT);

  pinMode(DIR, OUTPUT);
  pinMode(PW, OUTPUT);
  pinMode(encoder_outputA, INPUT);
  pinMode(encoder_outputB, INPUT);


  deviceState = STANDBY;

  digitalWrite(DIR, LOW); // this will brake, regardless of what ph is
  digitalWrite(PW, LOW);


}

void loop() {
  // put your main code here, to run repeatedly:
  float current = 0;
  float current_mA = 0;

 // int volt = analogRead(A2);
  // 10 for no syringe, 11 for syringe on, 12 for needle on
```

```
 // int stall = 10;
// float current= (volt+0.5) * (5.0 / 1023.0)*1000/40;
  buttonVal = digitalRead(button);
  float revolution = revo(count);
  Serial.print(revolution);
    Serial.print(",");
//  Serial.println(" rounds");
//  Serial.print(" ");
 // Serial.print(volt);
 // Serial.println(" ");
  current = ina219.getCurrent_mA();
      Serial.print(current);
    Serial.println();
// Serial.print("Current:       ");
// Serial.print(current);
// Serial.println(" mA");

  if (revolution > 0 || revolution <-60)
  {     digitalWrite(DIR, LOW);
      analogWrite(PW, LOW);}

  if(deviceState == STANDBY){
    if(buttonVal == HIGH){
      deviceState = CUTTING;
      digitalWrite(DIR, HIGH);
       analogWrite(PW, 255);
      delay(100);
    }
  }

  else if(deviceState == CUTTING){
    if(buttonVal == HIGH){
      digitalWrite(DIR, LOW);
      digitalWrite(PW, LOW);
      deviceState = REMOVAL;
      delay(100);
    }
  }

  else if(deviceState == REMOVAL){
    if(buttonVal == HIGH){
      deviceState = EXITING;
      digitalWrite(DIR, LOW);
      analogWrite(PW, 255);
      delay(100);
    }
```

```
  }

  else if(deviceState == EXITING){
    if(buttonVal == HIGH){
      digitalWrite(DIR, LOW);
      digitalWrite(PW, LOW);
      deviceState = STANDBY;
      delay(100);
    }
  }

  //Serial.print(deviceState);
  //Serial.print(" ");

  delay(100);
}

void CountA()
{
  if(digitalRead(encoder_outputB) == HIGH)
  {
    c=a;
    count--;
  }

  if(digitalRead(encoder_outputB) == LOW)
  {
    c=b;
    count++;
  }
  ppsA++;
}
```

LIST OF REFERENCES

[1] F. Bray, J. Ferlay, I. Soerjomataram, R. L. Siegel, L. A. Torre, and A. Jemal, “Global cancer statistics 2018: GLOBOCAN estimates of incidence and mortality worldwide for 36 cancers in 185 countries,” *CA. Cancer J. Clin.*, vol. 68, no. 6, pp. 394–424, 2018, doi: 10.3322/caac.21492.

[2] J. Ferlay *et al.*, “Estimating the global cancer incidence and mortality in 2018: GLOBOCAN sources and methods,” *Int. J. Cancer*, vol. 144, no. 8, pp. 1941–1953, 2019, doi: 10.1002/ijc.31937.

[3] L. Egevad, T. Granfors, L. Karlberg, A. Bergh, and P. Stattin, “Prognostic value of the Gleason score in prostate cancer,” *BJU Int.*, vol. 89, no. 6, pp. 538–542, 2002, doi: 10.1046/j.1464-410X.2002.02669.x.

[4] F. H. Schröder *et al.*, “Screening and Prostate-Cancer Mortality in a Randomized European Study,” *N. Engl. J. Med.*, vol. 360, no. 13, pp. 1320–1328, 2009, doi: 10.1056/nejmoa0810084.

[5] K. Hoyt *et al.*, “Tissue elasticity properties as biomarkers for prostate cancer,” *Cancer Biomarkers*, vol. 4, no. 4–5, pp. 213–225, 2008, doi: 10.3233/CBM-2008-44-505.

[6] P. Mao, K. Nakao, and A. Angrist, “Human Prostatic Carcinoma: An Electron Microscope Study,” *Cancer Res.*, vol. 26, no. 5, pp. 955–973, 1966.

[7] E. Özden, Ç. Göğüş, Ö. Tulunay, and S. Baltaci, “The Long Core Needle with an End-Cut Technique for Prostate Biopsy: Does It Really Have Advantages When Compared with Standard Needles?,” *Eur. Urol.*, vol. 45, no. 3, pp. 287–291, 2004, doi: 10.1016/j.eururo.2003.10.004.

[8] A. Barnett, P. W. McLaughlin, H. Zheng, and J. Z. Moore, “Novel Instant Vacuum Biopsy Needle System.” Aug. 04, 2013, doi: 10.1115/DETC2013-13028.

[9] P. Y. Wu, H. Kahraman, and H. Yamaguchi, “Development of aspiration-assisted end-cut coaxial biopsy needles,” *J. Med. Devices, Trans. ASME*, vol. 11, no. 1, pp. 1–9, 2017, doi: 10.1115/1.4035688.

[10] D. Ungurait, “Modification and Performance Analysis of an Aspiration-Assisted Prostate Biopsy Device,” M.S. thesis, H. W. College of Eng., Univ. of Florida, Gainesville, 2023.

[11] O. Valenzuela, I. Rojas, F. Rojas, and L. Marquez, “Automatic classification of prostate cancer using pseudo-gaussian radial basis function neural network,” *ESANN 2005 Proc. - 13th Eur. Symp. Artif. Neural Networks*, no. April, pp. 145–150, 2007.

[12] “25D Metal Gearmotors,” Polulu Robotics & Electronics, Aug. 2021. Available: https://www.pololu.com/file/0J1829/pololu-25d-metal-gearmotors.pdf

[13] Polulu Robotics & Electronics, “Pololu G2 High-Power Motor Driver 24v13,” www.pololu.com. https://www.pololu.com/product/2992

[14] D. J. van Gerwen, J. Dankelman, and J. J. van den Dobbelsteen, “Needle-tissue interaction forces - A survey of experimental data,” *Med. Eng. Phys.*, vol. 34, no. 6, pp. 665–680, 2012, doi: 10.1016/j.medengphy.2012.04.007.

BIOGRAPHICAL SKETCH

Yibo Wang was born and raised in Jinan, Shandong, China. He received a B.S. degree in Mechanical Engineering from Shijiazhuang Tiedao University, Hebei, China, in 2020. Then he moved to United State for further study and participated a joint program with Florida Institute of Technology. He graduated from Florida Institute of Technology in 2022 with a B.S. degree in Mechanical Engineering. During his undergraduate education, Yibo worked as a research assistant under the supervision of Dr. Pei Feng Hsu. He focused on the research of coating material and heat transfer efficiency, like coding and programming for thermal conductivity simulation. In addition, he also worked as a teaching assistant in the department of Mechanical Engineering.

After graduation from Florida Institute of Technology, Yibo moved to Gainesville and worked toward an M.S. degree in Mechanical Engineering at the University of Florida. In his first year of graduate school, he joined the Nontraditional Manufacturing Laboratory under the guidance of Dr. Hitomi Greenslet. He worked on the aspiration-assisted prostate cancer biopsy project, focusing on designing and manufacturing the handheld version of biopsy device. Yibo’s research interests include control, drone investigation and medical robots. He hopes to pursue a doctoral degree after graduation.